Received 22 June 2024; revised 30 August 2024; accepted 9 September 2024. Date of publication 12 September 2024; date of current version 22 November 2024.

Digital Object Identifier 10.1109/OJAP.2024.3459045

Through-the-Wall Human Activity Recognition Using Radar Technologies: A Review

JAWAD YOUSAF[1] (Senior Member, IEEE), SATANAI YAKOUB[1], SARA KARKANAWI[1], TAIMUR HASSAN[1] (Senior Member, IEEE), EQAB ALMAJALI[2] (Member, IEEE), HUMA ZIA[1] (Member, IEEE), AND MOHAMMED GHAZAL[1] (Senior Member, IEEE)

[1]Electrical, Computer, and Biomedical Engineering Department, Abu Dhabi University, Abu Dhabi, UAE
[2]Electrical Engineering Department, University of Sharjah, Sharjah, UAE

CORRESPONDING AUTHOR: J. YOUSAF (e-mail: jawad.yousaf@adu.ac.ae)

This work was supported by the Abu Dhabi University's Office of Research and Sponsored Programs and Research Institute for AI and Emerging Technologies, Abu Dhabi University, Abu Dhabi, UAE.

ABSTRACT Ultra-wideband radar technology (UWB) has demonstrated its vital role through various applications in surveillance, search and rescue, health monitoring, and the military. Unlike conventional radars, UWB radars use high-frequency, wide-bandwidth pulses, enabling long-range detection and penetrating obstacles. This work presents an in-depth review of UWB radar systems for recognizing human activities in a room and through-the-wall (TTW) with other diverse applications. After briefly discussing different UWB radar working principles and architectures, the study explores their role in various TTW applications in real-world scenarios. An extensive performance comparison of the legacy studies is presented, focusing on detection tools, signal processing, and imaging algorithms. The discussion includes an analysis of the integration of machine learning models. The primary focus is on the detection, movement, monitoring of vital signs, and nonhuman classifications in the context of Through-The-Wall (TTW) scenarios. This study contributes to a better understanding of evolving technology capabilities by integrating artificial intelligence (AI) and robotics to automate and precisely locate the target in various scenarios. Furthermore, the discussion includes the impact of UWB technology on society, future industry trends, the commercial landscape, and ethical issues to understand and future research.

INDEX TERMS Ultra-wideband (UWB) radar, IR-UWB radar, CW-UWB radar, through-the-wall (TTW) detection, human motion, human presence, signal processing, machine learning, and convolution neural network (CNN).

I. INTRODUCTION

MODERN and innovative technological breakthroughs have prompted an increase in demand for smart systems. Such advancements provide a multitude of benefits, focusing on enhanced accuracy and operational capabilities, eliminating the need for human intervention. Among the diverse approaches, radar-based solutions have become an increasingly prevalent method for intelligent systems [1], [2], [3]. The employability of radar technology provides versatility in identifying diverse targets in a variety of applications and sectors. As a result, radar-based automation is more durable and precise, allowing for the integration of intelligent technologies in modern society [4], [5], [6], [7].

Radars are detection devices that emit electromagnetic wave to recognize the characteristics of an item based on the backscattered signals from the target [8], [9], [10], [11]. The emergence of ultra-wideband radar (UWB) topology has recently gained prominence due to their applications in adverse environments of surveillance, search and rescue, agricultural, manufacturing industry, health monitoring, military fields and indoor localization as depicted in Figure 1 [1], [2], [3], [7], [12], [13], [14], [15]. Conventional radar systems employ limited frequency array and waveforms based on harmonics.

UWB radar systems, on the other hand, rely on brief chirps transmitted at wide frequency bandwidths [11], [16],

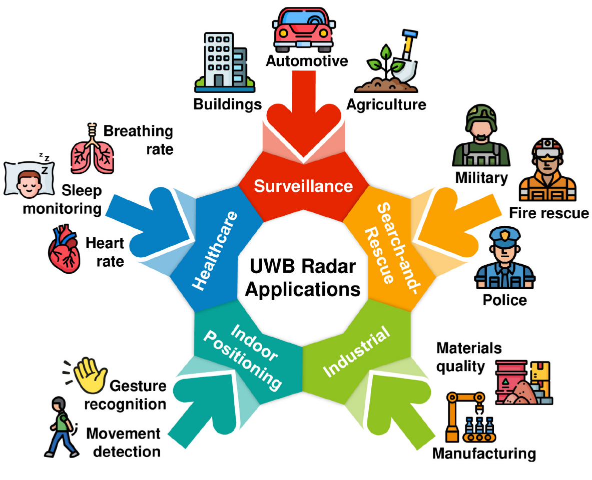

FIGURE 1. Practical real-world applications of UWB radar technology.

[17], [18]. The ultra-short time domain pulse is comprised of fast falling and rising edges enabling fine timing resolution at the receiver end. Its radio frequency (RF) extends over a large spectrum that can be designed to emit signals that appear as imperceptible random noise. This unique characteristic enables both long-range detection and penetration through materials. Researchers have adopted this wide frequency range feature for through-the-wall (TTW) applications as it can determine the composition of a target with minimal information loss [19], [20], [21]. Furthermore, its employment in real-time applications has been proven to be practical due to its ability to discern intended targets without the need for the target to be equipped with an RF source [22], [23], [24], [25], [26].

Figure 2 represents the general working principle of UWB radars. A signal is transmitted from the UWB transceiver toward a target present behind a wall. The received signal is the sum of all reflections captured by the receiver. Various kinds of signal processing and denoising techniques are applied to the backscattered raw signal for feature extractions [8], [9], [27], [28], [29]. The classification of human or non-human object activities and vital signs monitoring is performed based on post-processed signals by either conventional or machine learning models for a wide range of real-world applications [20], [21], [27], [30], [31], [32], [33], [34].

Artificial intelligence and robotic systems permeating society are advancing technology and various industries. This advancement is centered on rapidly detecting and recognizing targets at a high precision rate whilst simultaneously discerning its environment for intelligent conclusions by integrating radar sensors with AI and robotic devices [13], [14], [35]. An artificially intelligent robot equipped with a UWB radar sensor for TTW detection will be able to recognize situations and make judgments autonomously and sufficiently [25], [26], [36]. Such systems are developed using machine learning algorithms that have predominantly been based on conventional neural networks (CNN) by integrating radar sensors with AI and robotic devices. The emergence of machine learning algorithms offers a flexible approach to modeling systems as they can be automatically applicable under various environments based on its redundant patterns [20], [32]. The development of a trained radar-equipped robot ensures the operator's safety when performing rescues without compromising its efficiency in detecting targets by integrating radar sensors with AI and robotic devices.

This study serves as a guide for the basics as well as advancements in UWB radar systems for TTW human detection and recognition applications with and without AI integration. It expands to provide readers witha comprehensive information related to the different radar sensors, applications, processing methods, and machine learning advancements in the field. A revolving discussion about the advancements and limitations of various UWB techniques for the subject applications with an in-depth review of legacy studies is presented. A brief introduction to radar (UWB, IR, CW) technologies for detection and vital signs monitoring applications is presented in Section II. The preceding sections examine the radar structure, operation, and signal pre-processing methods. Section II-A discussed the various approaches for the recognition of human activities (walking, sitting, moving away, and towards the radar sensors) TTW [25], [26], [36], [37], [38], [39] and detection of human presence and vital signs without any obstructions such as walls [33], [40], [41] using UWB radar sensors. The details of various kinds of commercial [27], [32], [42], [43], [44], [45], [46], [47], [48] and customized [20] impulse (IR) UWB radar sensors used for human activity recognition (presence [27], [42], [43], [48], motion [20], [32], [44], [46], [47], sleeping postures [45], [46], [47], and breathing [27], [42], [46]) in with [20], [32], [42], [43] and without walls [27], [44], [45], [46], [47], [48] environments are given in Section II-B. The use cases of various self-developed frequency-modulated continuous-wave (FMCW) radar for human presence [28], [49], [50], [51] and motion tracking [21], [24], [28], [52] with different signal processing algorithms and various wall thicknesses are described in Section II-C. An extensive comparison of various features and capabilities of key commercially available UWB [53], [54], [55], [56], [57], [58], [59], IR-UWB [60], FMCW [61], [62], and microwave [63], [64] sensors is presented in Section III. Section IV extensively discussed and compared the deployment of various machine learning techniques along with UWB radar technologies for the detection and characterization of human motion [20], [26], [26], [36], [37], [38], [44], [45], [46], [47], presence [41], [43], [48], [51], [65], [66], [67], [68], and vital signs [8], [10], [11], [27], [28], [29], [30], [31] along with non-human objects [22], [23], [33], [34], [69], [70]. Lastly, future research trends are discussed in Section VI. Table 1 summarizes the reviewed studies based on the detection and characterization of various classes.

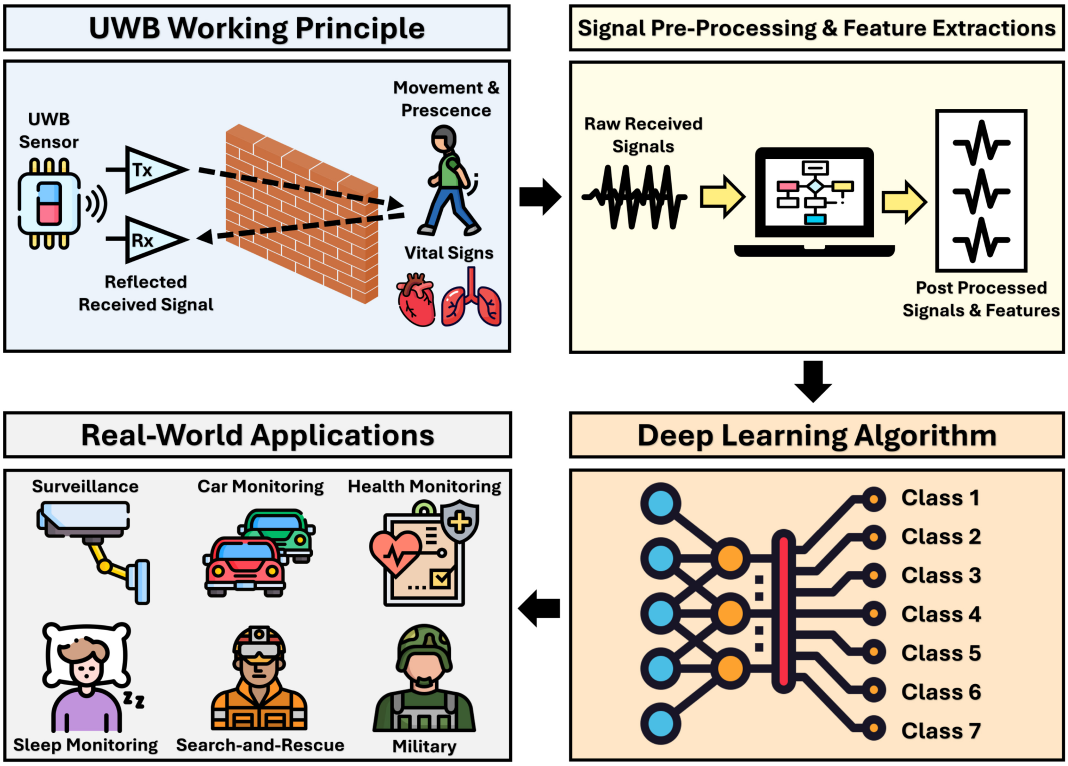

FIGURE 2. UWB radar data processing, classification, and application potential.

TABLE 1. Summary of reviewed studies for human/non-human detection and vital sign characterizations using UWB radar technologies.

Detection Application	References
Human Presence	[28], [32], [37], [41]–[45], [48], [50]–[52], [65]–[68], [71]–[73]
Human Presence & Vital Signs Analysis	[8]–[11], [17], [18], [27]–[31], [39], [40], [42], [74]–[83]
Human Activity Recognition	[18], [20], [21], [24]–[26], [28], [32], [36]–[38], [41], [43]–[49], [73], [84], [85]
Non-Human Presence	[8], [22], [23], [33], [34], [69], [70], [86]

II. RADAR TECHNOLOGIES FOR DETECTION APPLICATIONS

An UWB radar's receiver relies on the shortest line-of-sight path which can be easily distinguished due to the short pulse duration. Over the years, UWB radars have been enhanced further, with research focusing on impulse radar ultra-wideband (IR-UWB) and continuous wave (CW) UWB radar systems [20], [21], [24], [32]. Regardless of the selected approach, UWB radar sensors have applications in security and surveillance systems because of their ability to pierce obstacles and identify targets at large distances. Such characteristics are critical for operational uses in rescue missions and counter-terrorism, where reducing injuries and fatalities is imperative [72], [76]. Also, the use of UWB has advanced and expanded in fields related to healthcare where the transmitted signal can pierce the human body without causing harm, cultivating radar-based non-wearable devices [77], [78], [79], [80], [81], [87]. Table 2 presents a general comparison of various radar technologies.

A. ULTRA-WIDEBAND (UWB) RADAR

Through-the-wall detection of motion and presence may be identified by utilizing various methods of radar imaging. Most famously, UWB radars are commonly equipped in such applications due to their ability to effectively permeate through the walls. Unlike traditional narrowband radars, which have a limited frequency range, UWB radars transmit a wide range of electromagnetic waves as shown in Figure 3. These UWB chirp signals can penetrate obstacles such as walls, and the backscattered signal contains the signature information of the target. As a result, proper target composition is possible while critical information is preserved and losses are minimized.

Figure 4 shows a typical backscattered radar signal waveform in the time domain. The first sharp high-amplitude spike represents the coupling between the transmitter (Tx) and receiver (Rx) antennas of the radar. The amplitude of this spike depends on the placement, orientation, and distance between the Tx and Rx antennas of the radar modules. The reflection from the obstacle like a concrete wall is

TABLE 2. Comparison of the various radar technologies different applications.

Radar Technology	Significance	Difficulties	Advantages
UWB (Ultra-Wideband) [25], [26], [36]–[39]	• High spatial resolution • Highly effective for TTW detection • Higher accuracy in complex environments	• Short detection range • Hardware is often costly and complex	• Penetrate various materials and obstacles • Low power consumption • Effective performance in cluttered environments
IR-UWB (Impulse Radio UWB) [32], [42], [46]–[48], [60]	• Excels in cluttered environments • High accuracy for detecting small movements	• Complex signal processing • Susceptible to noise disruptions	• Generally cheaper hardware as compared to UWB • Effectively penetrates through multiple materials and obstacles
Microwave [63], [64]	• Provides real-time feedback and monitoring • Effective over long distances	• Less effective at penetrating through solid objects • Large system for high-frequency applications	• Reliable and robust • Various applications such as traffic monitoring and meteorology
FMCW (Frequency Modulated Continuous Wave) [28], [49], [61], [62]	• Continuous operation and real-time data • Accurate distance and velocity measurements	• Complex signal processing • Less effective for detecting small movements	• Works well in different weather conditions • Particularly good for measuring speed
SFCW (Stepped Frequency Continuous Wave) [50], [51], [88], [89]	• High-resolution measurements • Effective for detecting targets with precision	• Frequency stepping is time-consuming • Limited real-time performance	• High accuracy and resolution over a wide range • Cost-effective for specific applications

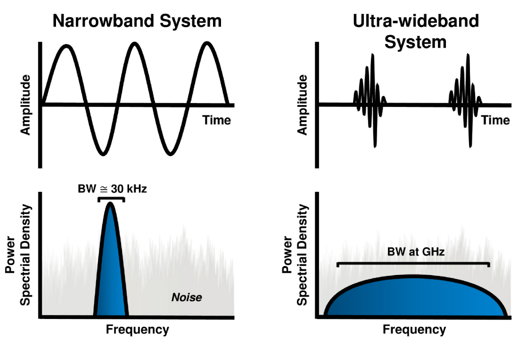

FIGURE 3. Narrowband vs. UWB signals in time and frequency.

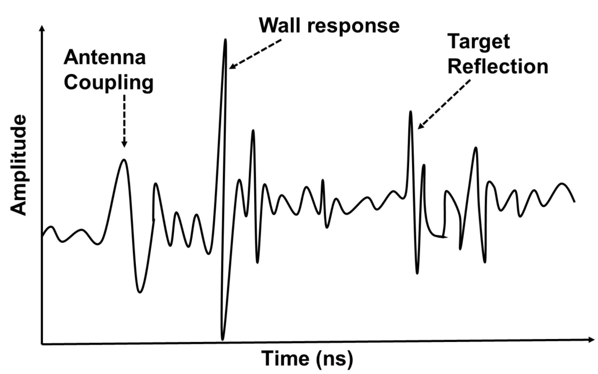

FIGURE 4. Typical UWB radar backscattered response signal in time domain.

observed in terms of the second high spike in the returned captured signal by the radar Rx antenna [32], [41], [45], [72], [73]. The target (human or non-human object) signature information is contained within the spikes after the wall responses as shown in Figure 4. The amplitude and sharpness of this reflection depend on the type and movement of the target object. The amplitude level of these spikes also varies with the change in the radar unit properties [43], [48], [51], [52]. For example, for the commercial SLMX4 [60] radar sensors, the first spike in the raw radar signal has the highest peak (representing very strong antenna coupling) , and afterward, spike amplitude is lower.

Methods for visualizing radar data include various domains that fall under target imaging. This technique enables the prompt monitoring and detection of targets by leveraging the physical parameters of the observed objects. The increase in wireless systems has impacted radar transmission due to interference from surrounding electromagnetic waves, leading to challenges in acquiring, transmitting, and processing data. Consequently, this has resulted in data sparsity, leading to complications and ineffective radar operation [90]. To address these challenges, a radar target imaging technique based on compressed sensing (CS) has been developed, allowing for the reduction of echo data while maintaining imaging quality. Unlike conventional methods bounded by the Nyquist sampling theorem, CS exploits the sparse characteristics of the target's scattering distribution. Coefficients are then derived for the construction of a measurement matrix that enhances the target imaging quality and the data down-sampling rate [91].

The analysis of both one-dimensional (ID) *i.e.,* time domain signals [25], [26], [32], [37], [38], [40], [41], [42], and two-dimensional (2D) signals *i.e.,* scalograms or spectrograms [30], [33], [36], [38], [40] is performed to extract the target features such as presence, movement, and vital signs. The returning signals from radar systems from moving targets contain time-varying information across the time and frequency domains. To optimally analyze this data, a joint representation is employed using time-frequency analysis [92]. This is often achieved based on methods such as the continuous wavelet transform (CWT) for generating scalograms, or the short-term Fourier transform (STFT) for the construction of spectrograms. With additive processing, these representations enhance the ability to localize and track targets and can also serve as input for various algorithms. The precise classification of the target class (es) is achieved by training the artificial intelligence (AI)–powered algorithm on extracted feature data.

The studies [25], [26], [36], [37], [38], [39] employ UWB techniques to establish the identification of motion behind a brick wall. In a controlled experimental environment, a signal with an operating frequency of less than 2.5 GHz is transmitted. The received signals are commonly impeded by the effects of noise or objects occupying the environment. To mitigate such occurrences, [25] [33] employs the method of background subtraction after pre-processing the returned signal. This is accomplished by taking the difference between the current frame and a reference frame, resulting in an identifiable background [93]. However, this method lacks robustness for various factors. High accuracy can be achieved strictly when the speed of movement of the object is occurring at a substantially high threshold. Furthermore, pixelated instances may impede and blur the boundaries between background and foreground objects, making the identification of real motion difficult [93]. While similar methods for background removal have been presented and additive pre-processing methods such as direct coupling suppression [39] and least mean square [25], [39] are used, and computational and storage capacity is compromised. When researchers employ this strategy, a visual reconstruction of the signal is supplied as input to the machine learning algorithm rather than the signal itself. Doing so runs the risk of increasing the computational burden of the established algorithm.

Alternative methods of signal processing and feature extraction have been utilized by other researchers. Authors in [26], [37], [38] experimented with identifying human motion and breathing rate through an approximately 20 cm thick brick wall by transmitting a signal in the time domain. The processing methods taking place include Hilbert-Huang transform (HHT), Gaussian measurement, fast Fourier transform (FFT), and S-transform (ST), respectively. The success of different processing methods is established for each research and its intended applications based on their ability to minimize noise. While FFT is extensively used, it introduces limitations as it requires a linear processing unit. One may argue that real systems perform almost linearly under certain conditions. However, the system's linearity is destroyed as the time increases or the operating conditions are changed [94]. Additionally, the FFT is known to decompose signals into harmonic components which leads to spectrum expansion, particularly for non-stationary signals. As a result, signals in the frequency domain are misinterpreted.

Alternatively, the Hilbert-Huang transform (HHT) was introduced as a non-linear processing method. Its purpose is to determine the instantaneous frequency by utilizing the empirical mode decomposition (EMD) on a set of internal mode functions (IMF) [94]. In [26], the HHT was used to display the signal data in a range-time map (RTM). This resulted in a set of images that were utilized as inputs to their suggested machine learning algorithm, which yielded a 93.06% accuracy. The signal processing method in [38] found that a clearer depiction of the breathing rate of recognized human movement was evident when representing its signals in ST rather than FFT analysis, as seen in Figures 5(a) and 5(b) respectively. However, the use of HHT was opted out as it cannot appropriately represent specific qualities in their research as its classification of vital signs is inaccurate.

Detecting vital signs can be achieved for both respiration and heart rates with the processing of a backscattered UWB radar signal. A breathing target will experience periodic motion over a certain interval. The change of frequency usually falls within a range of 0.2-0.5 Hz, and the heartbeat rate at a frequency window of 0.8-3.3 Hz [95]. The presented work in [30], [38], [40] employs the use of UWB radar to detect human presence and vital signs. The breathing conditions bradypnea, eupnea, and tachypnea are retrieved from humans breathing steadily at a fixed posture [38]. Their respective frequencies are 0.25 Hz, 0.35 Hz, and 0.7 Hz. Eupnea refers to the pattern exhibited at a mean respiration rate per minute (rpm) ranging from 12 and 16. The bradypnea pattern is usually exhibited at an increased respiration cycle which falls ≤ 12. Finally, tachypnea has a mean rpm that is ≥ 16 which occurs in instances of weakness or normal health conditions but strains on the normal health condition due to light exercise [31]. The UWB radar proved more precise in identifying the human's weak life signs, tachypnea, for its greater signal-to-noise ratio (SNR). As a result, the tachypnea signal was decomposed in time and

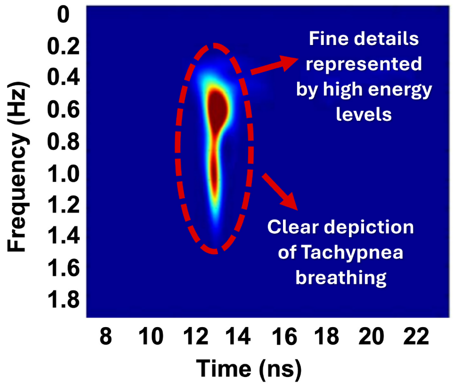

(a) S-transform (ST)

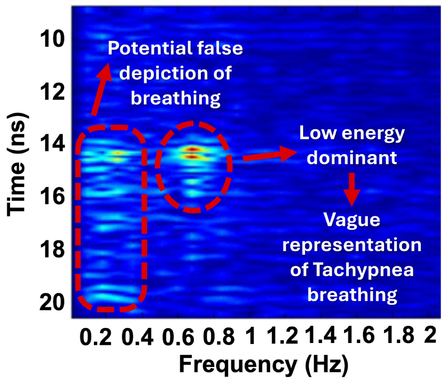

(b) Fast Fourier transform (FFT)

FIGURE 5. Tachypnea vital sign analysis [38].

frequency domain to obtain its frequency characteristics for the extraction of periodic motion and target location as depicted in Figures 5(a) and 5(b) using ST and FT approaches, respectively.

A vital sign detection method based on P-times extraction is proposed in [40]. Based on the aforementioned vitals frequencies, cyclical fluctuations of the chest cavity approximating to sinusoidal signals during contraction and relaxation are exhibited. Following the pre-processing method, the proposed P-times algorithm is applied to extract respiration and heartbeat information of the trapped person. This method is based on the energy of the slow time slice defined in Figure 1, with an energy window width of 3.

$$e_n = \sum_{m=1}^{M} |f_{(m,n)}|^2 \tag{1}$$

In the above equations, $f_{(m,n)}$ is the amplitude of the mth row and nth column in the matrix, and e_n is the energy of the nth slow time slice that accumulates to produce total energy $E_n = \sum_{n-1}^{n+1} e_n$ [40]. The information about the exhibited vital signs fall under 4-6 slow time slices. Slow time in terms of radar applications is the time dimension when the radar measurements are taken over multiple pulses. The base time length and step length are set to two seconds for extraction of P times as inhalation and exhalation rates fall under the selected time. The frequency and amplitude information of each time slice is synthesized to achieve the maximum average amplitude.

Machine learning algorithms have emerged as potential candidates to address the limitations of the conventional techniques used in [26], [37], [38], [40], [94], [95]. In [30], a hear-monitoring convolutional neural network (CNN) system is developed for the estimation of heart inter-beat intervals (IBI). This is achieved with a combination of electrocardiogram (ECG) devices and UWB-based radar data. The user must first register their name and user ID before attaching the ECG electrodes to their chest. However, the reported system has limitations since it is device-driven and can only monitor certain users under static conditions. The requirement that the device be attached to the user to provide reliable test results may also be inappropriate for certain patients, such as the elderly, infants, and burn victims. Infants and patients suffering from burns may experience movement restrictions and are more vulnerable to secondary injuries [82]. Furthermore, the acquisition of user data through the registration system may result in a breach of user privacy. Alternatively, the study by [82] presented a device-free UWB radar-based respiration and heart rate monitoring system. Respiration and heart rate signals are extracted independently and denoised for further analysis using a wavelet threshold basis function. Because it is based on a variable analysis window of temporal frequency, the wavelet transform is effective in determining the resolution of a signal over a broad frequency scope. Its wide window can be used to identify low-frequency signals, while its narrow window can be used to analyze high-frequency signals [96]. A critical comparison of reviewed studies based on UWB radar technology is depicted in Table 3.

B. IMPULSE ULTRA-WIDEBAND (IR-UWB) RADAR

This section discusses the legacy studies that employed impulse radar ultra-wideband (IR-UWB)–based systems for various human detection and monitoring applications. Signals produced by this radar technology can tolerate the effects of interference, resulting in an increased time-of-flight (ToF) resolution. This, in turn, enables an efficient mechanism ideal for ground-penetrating and short-range radars capable of detecting hidden targets behind walls using IR-UWB time domain signals [20], [27], [32], [42], [43], [44], [45], [46], [47], [48].

The studies in [20], [32], [42], [43] seek to detect human presence through a wall. Three analytical approaches are used to identify the presence as well as breathing signals of detected humans in [42]. The breathing motion of a stationary human will create periodic fluctuations due to small chest movements, as portrayed in Figure 6. The first pre-processing method eliminates static clutter. A difference square matrix is constructed by computing the difference between scans. In the second analytical approach, the moving average reference is applied by subtracting the cumulative

TABLE 3. Comparison of reviewed studies using UWB radar technology for diverse applications of without and through-the-wall (TTW) cases.

Technology	Ref	Year	Detection Machine	Processing Domain	Frequency Range	Signal Processing	TTW	Wall Material (Thickness)	Target Application (s)
UWB	[25]	2022	Self developed	Time	0.5-2.5 GHz	Least mean square Background subtraction	Yes	Double layer concrete (0.23m)	Human motion (7 different types)
	[36]	2020	Self developed	Frequency	1.6-2.2 GHz	Moving target indicator	Yes	Brick (0.70m)	Human motion (boxing, walking, picking, and raising arms)
	[26]	2022	Self developed	Time	0.5-2.5 GHz	Moving target indicator Averaging of matrix (doppler-time map) Time-domain gating & Hilbert-Huang (range-time map)	Yes	Double layer concrete (0.23m)	Human motion (7 different types)
	[37]	2016	PulsON410	Time	n/a	Compressed detection algorithm (gaussian measurement)	Yes	Brick (23.5cm)	Human motion (one person, periodic swinging of arms, two people)
	[38]	2012	SIR-3000	Time	1-4 GHz	2D-FFT S-transform	Yes	Brick & plaster coating (0.2m)	Human motion & breathing
	[39]	2021	UWB radar	n/a		Normalization Low-pass filter DC suppression Wavelet entropy Least mean square Range accumulation Correlation coefficient	Yes	Concrete (53cm))	Distinguish breathing of humans from animals
	[33]	2021	UWB radar	n/a		Image generation Radar cross section Background subtraction	No		Identification of 7 types of drones
	[40]	2021	Self developed	Time	0.85-9.55 GHz	Butterworth filter P-times extraction Linear error correction Linear trend suppression Cumulative noise distribution	No		Vital signs
	[30]	2019	MIMO UWB Radar	Time	n/a				Human presence & vital signs
	[41]	2022	Mobile UWB Sensor	Frequency	n/a	Feature extraction: time & power vectors	No		Human presence

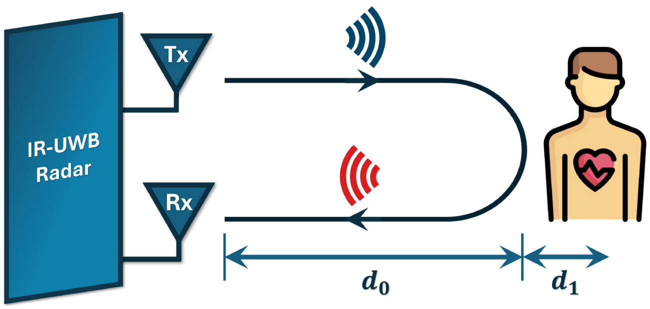

FIGURE 6. Schematic diagram of the radar detection principle. The time-of-flight of the pulse depends on antenna distance, d_0.

and average reference waveforms to decrease clutter. This improves the accuracy with which breathing patterns and motions are recognized. To detect targets, the final strategy adopts an HHT-based algorithm. The experimental results showed that the normalized difference and moving average reference technique can detect persons 6 ft and 3.2-4.0 ft away from the UWB radar, respectively. However, the application of the HHT approach could only detect the presence of human targets while ignoring their position and distance information. This is because the HHT approach relies exclusively on the spectrum features of the detecting signals, while range information is neglected.

Zhenglian et al. [20] proposed a CNN-based human motion status recognition system. While the resulting algorithm achieved a recognition accuracy rate of 99.7%, the simulated experiment includes factors that may impair the final results. The researchers assumed that the transmitted signal was not attenuated during propagation. In truth, no transmitted signal is immune to noise, especially when traveling long distances and traversing obstacles that decrease the signal-to-noise ratio (SNR). The SNR is weakened further as the experiment is carried out to detect targets hidden behind a wall.

The reduction of attenuation in noisy real-time environments has been practiced by [44] through five signal pre-processing methods: DC suppression, clutter suppression, matched filtering, signal resizing, and pulse-wise normalization. According to [12], matched filtering is an optimization technique intended for maximizing the SNR. Noise signals decrease the performance of radar systems by increasing the likelihood of generating false alarms. The filter receiver of $h_m(t) = s_m(T - t)$ is based on an impulse response that is the time-reverse of the input wavelet with period. By correlating the received signal to the impulse response, the components of the received signal that match the reference signal are enhanced while contrasting characteristics are attenuated. This response enables effective waveform design and assessment of UWB radar performance. Table 4 compares the reviewed studies on this technology.

TABLE 4. Comparison of reviewed studies using IR-UWB radar technology for diverse applications of without and through-the-wall (TTW) cases.

Technology	Ref	Year	Detection Machine	Processing Domain	Frequency Range	Signal Processing	TTW	Wall Material (Thickness)	Target Application (s)
IR-UWB	[42]	2014	PulsOn220	Time	n/a	Normalization; Empirical mode decomposition (HHT); Reference moving average (DFT)	Yes	Gypsum (33.02cm); Wooden door (10.16cm)	Human presence & breathing
	[32]	2023	Novelda X1	Time	0.45-3.55 GHz	CNN model (feature extraction)	Yes	Plywood (4.5cm)	Human motion
	[43]	2016	PulseOnP210	Time	2-6 Ghz	n/a	Yes	n/a	Human presence
	[20]	2021	Self-developed	Time	n/a	Average processing (of samples)	Yes	Brick concrete (0.2m)	Human motion
	[44]	2022	X4M03 Novelda	Time	n/a	Signal resizing; DC suppression; Matched Filtering; Clutter suppression; Pulse-wise normalization	No		Human motion (standing, walking, jogging, sudden swings, running)
	[45]	2023	Novelda XeThru X4M03 v5	Time	n/a	DC suppression; Background subtraction	No		Four different sleeping postures
	[27]	2019	NVA6201 Novelda	Time	n/a	Band-pass filter; Fast fourier transform	No		Human presence & breathing
	[46]	2020	PulsOnP440	Time	3.1-4.8 GHz	Band-pass filter; Background subtraction; Statistical parameters (skewness, kurtosis, power)	No		Human motion (walking, standing up, sitting down, lying down, & falling) & breathing
	[47]	2021	Novelda XeThru	Time	7.25-10.2 GHz	n/a	No		Human motion (5 different bed postures)
	[48]	2023	Novelda XeThru X4M02	Time	7.25-10.2 GHz	n/a	No		Human presence in cars

C. CONTINUOUS WAVE (CW) ULTRA-WIDEBAND RADARS

The continuous-wave (CW) radar visualizes detailed target information through Doppler maps, however, is limited in its inability to identify the target's range. To address this, researchers have investigated modified frequency modulated continuous wave (FMCW) and step frequency continuous wave (SFCW) techniques. Such techniques utilize simple continuous sinusoidal signals while depicting target range measurements [97].

TABLE 5. Comparison of reviewed studies using CW radar technology for diverse applications of without and through-the-wall (TTW) cases.

Technology	Ref	Year	Detection Machine	Processing Domain	Frequency Range	Signal Processing	TTW	Wall Material (Thickness)	Target Application (s)
CW	[51]	2019	UWB - SFCW	Frequency	2-4 GHz	IFFT	Yes	No wall Brick wall (145mm) Drywall (62.5 mm).	Human presence & posture (sitting down & standing up)
	[50]	2019	UWB-SFCW self developed	Frequency	0.5-2.5 GHz	CC-TDBP DC suppression Background subtraction	Yes	Brick & concrete (22.5cm)	Human presence
	[21]	2012	UWB-FMCW self developed	Frequency	2-4 GHz	Range gating Frame-to-frame coherent change detection	Yes	Concrete (10cm & 20cm) Cinder-block	Human motion
	[24]	2012	UWB-FMCW self developed	Frequency	1-4 GHz	n/a	Yes	Plasterboard	Human motion
	[28]	2015	FMCW self developed	Frequency	5.5-7.2 GHz	Iteration Successive silhouette detection Successive silhouette re-mapping Successive silhouette cancellation	Yes	Hollow wall w. steel frame (6in)	Human presence & tracking, breathing, 3D pointing
	[49]	2018	FMCW self developed	Frequency	n/a	Low-pass filter Fourier transform	Yes	Concrete (0.3m)	Human motion
	[52]	2022	FMCW self developed	Frequency	0.5-3 GHz	n/a	No		Human presence

The FMCW topology of continuous wave ultra-wideband radars have been applied in many studies for the TTW human motion recognition and vital signs analysis using frequency domain radar imaging as summarized in Table 5. By transmitting a wideband electromagnetic wave in the frequency domain towards the wall, a reflected signal consisting of the energy radiated is returned. FMCW-based systems for the detection of human presence and motion are reported in [28], [49], [52]. WiTrack 2.0, a proposed system in [28], is a multi-person localization framework that aims to detect human presence in cluttered indoor environments. This is accomplished by capturing the reflections of wireless signals emitted by the target's body.

Different reported legacy studies have succeeded in identifying human motion for a single person. Because one person is occupying the environment, all reflections are presumed to be the consequence of the target. A large number of people might be present in a real-time environment which makes it hard to distinguish different targets with multiple reflections. Adib et al. [28] overcome this by measuring the time of flight (ToF) from the constructed radar systems using multiple transmit-receive antenna pairs. The reflected signal in radar systems is a delayed replica of the transmitted signal, as shown in Figure 8. The ToF can thus be retrieved by taking the FFT of Figure 2.

$$ToF = \frac{\Delta f}{slope} \tag{2}$$

A problem known as near-far emerges when working with ToF profiles acquired from several Tx-Rx pairings. That is, humans close to the radar are more powerful than reflections of people further from the wall. To address this, the profiles are preprocessed using a successive silhouette cancelation (SSC) process. This first determines a user's strongest reflection by superimposing the 2D heat maps of the Tx-Rx pairs. The individual's location is then mapped, and the influence of the individual is minimized to identify a single target. Finally, the procedure is repeated for each ToF profile produced by every Tx-Rx combination to achieve the presented profiles in Figure 7. As a result, additional Tx-Rx antenna pairs can enhance target imaging quality. However, it is important to balance the desire for higher image resolution with the potential trade-off of bulkier hardware.

An FMCW-based custom radar system for TTW motion detection is discussed in [49]. The created system consists of two horn antennas designed to prevent multiple reflections. The goal of such a system is to address the issue of path losses caused by mounting radar system antennas directly on the wall. Raw data acquired from the transmitted and received signals is processed sequentially through time zero correction, DC removal, and FFT. While the overall system is capable of determining targets through 20-30 cm concrete barriers, the system is susceptible to interference and inaccurate distance estimations, both of which degrade the overall performance.

Additionally, solely relying on FMCW-based applications may introduce further challenges. As stated earlier, FMCW transmits waves towards the highest concentration of energy

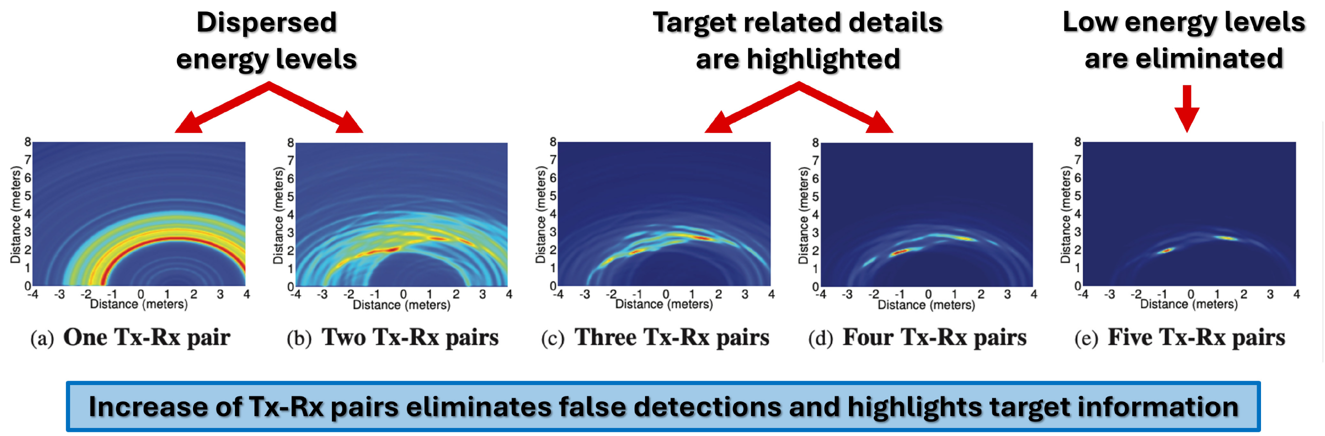

FIGURE 7. Localizing multiple users using the heatmaps obtained from combining ToF profiles of multiple Tx-Rx antenna pairs [28].

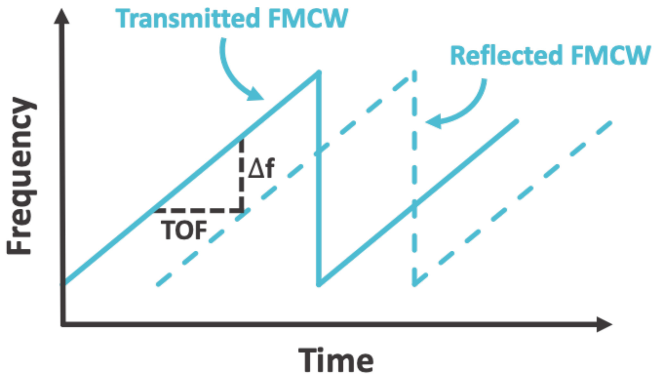

FIGURE 8. Transmitted FMCW signal and its reflection.

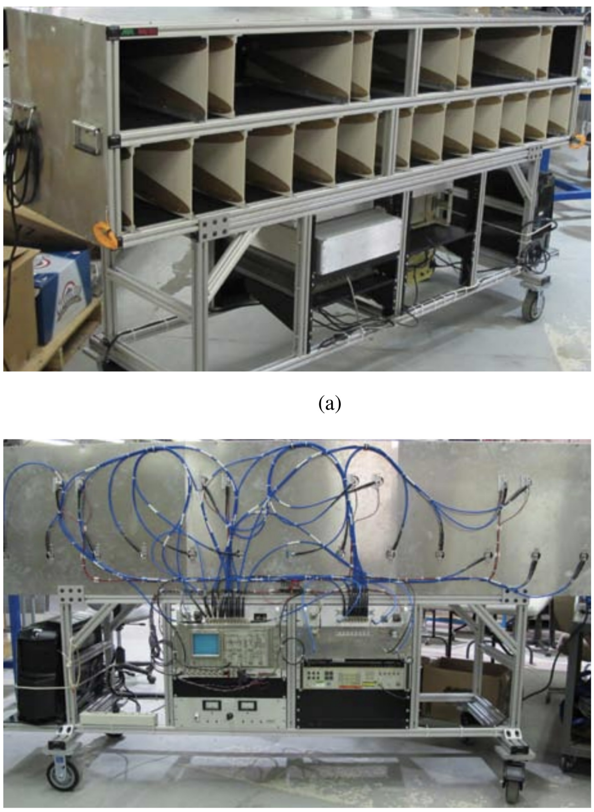

(a)

(b)

FIGURE 9. Photographs of the through-wall radar imaging system show (a) the antenna elements on the front of the system. (b) the transmitter, receiver, power supplies, diagnostic oscilloscope, and computer on the back [21].

and is then reflected to the radar. However, due to permittivity contrast and radar cross section, wall reflections are prone to masking the return of the target [49]. Recent studies [21], [24], [50], [51], have chosen to combine UWB and CW devices to mitigate the effect of wall reflections. Relatively low frequencies can easily penetrate walls in UWB systems due to broad wavelengths and lower wall losses that are proportional to frequencies. Meanwhile, high frequencies produce an appropriate resolution of the captured radar images.

Alternative FMCW systems based on UWB radars have been reported in [21], [24]. For TTW imaging, [21] devised a system that employs an S-band FMCW radar. S-band radars have a frequency range of 2.9 to 3.1 GHz [98]. The use of this frequency scope enables the effective propagation of electromagnetic waves through walls. The detection of moving and stationary targets in free space, behind 20 cm concrete walls, determined the efficacy of the chosen radar topology. Range gating and frame-to-frame coherent change detection are used to remove clutter [99]. As a result, the dynamic range of the system is increased, and weaker targets occluded by walls are efficiently recognized. Range gating is an effective processing method for FMCW systems. Because both the receiver and transmitter run concurrently in FMCW systems, the dynamic range of the system is limited [100]. While research has demonstrated the reliability of S-band radars for TTW detection, their practicality is limited. S-band radars necessitate several antennae to maximize frequency bandwidth, as illustrated in the system proposed by [21] in Figure 9. These systems are not cost-effective and are often designed at a large scale [98], [101]. Furthermore, traversing

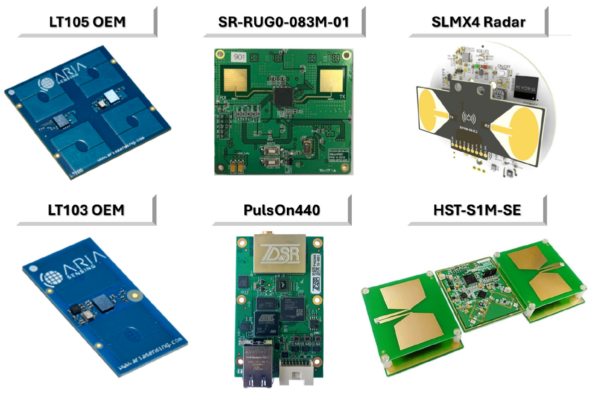

FIGURE 10. Commercial UWB radar sensors used for diverse applications [53], [54], [55], [56], [58], [60].

a complicated device is impractical for indoor environments and applications of rescue, search, and security missions.

To leverage the benefits of FMCW radar systems, researchers have alternatively investigated SFCW radars for their ability to create low-power, robust, and compact systems [88]. However, due to the radar's parameters and characteristics, SFCW radars are most optimal for short-range detection. Using an SFCW radar, authors in [97] analyzed the respiration rates in multiple stationary targets. This was accomplished using a homodyne SFCW radar operating at a center frequency of 3 GHz and a bandwidth of 2 GHz. This facilitates TTW detection while maintaining the radar's range resolution. A two-stage algorithm was proposed to determine target range and Doppler profile extraction. Experimental results demonstrated the method's capability to detect single targets. Additional tests with volunteers spaced 1 m to 30 cm apart showed that the radar was able to differentiate between multiple individuals, although ghost targets were also triggered during the experiments.

For enhanced range resolution, Su et al. combined an SFCW radar with a self-injection locked (SIL) radar to develop a single-conversion stepped frequency continuous-wave (SCSFCW) radar [89]. While FMCW and SFCW are notoriously known for their ability to present both range and Doppler information, their performance is limited by susceptibility to noise, restricted range, and low sensitivity. With the integration of SIL radar, these limitations are addressed as vital signs are extractable by providing high Doppler sensitivity [89]. The experimental setup taking place consists of a human target seated approximately 4 m from the radar. Researchers observed that a range beyond this distance poses challenges when detecting and extracting respiration and heart rates. To evaluate the system's range resolution, two volunteers were placed at varying distances. Both the range and Doppler spectra of the radar data were used to identify the target's position. The results indicated that the radar was unable to discern or identify targets located less than or equal to 30 cm apart. The experimental set-up takes place with three stationary targets placed within the line of sight of the Tx-Rx antenna, ensuring no overlap between the targets. Peaks in the range and Doppler spectra corresponded to the location of the targets, which were further processed into range-Doppler maps (RDM) for the visualization and tracking of vital signs. However, this method relies on detecting local peaks using a predetermined threshold, which may not be applicable in circumstances where the target has engaged in activities that significantly alter their respiration or heart rates.

III. COMMERCIAL RADAR SENSORS FOR DIVERSE APPLICATIONS

Despite the development of customized radar sensors for various applications by researchers, a variety of commercial radar sensors are also deployed for a wide range of human activity and health care monitoring applications. Table 6 provides an extensive comparison in terms of operating frequency, bandwidth, beamwidth, detection range, and potential applications of key commercially reviewed UWB [53], [54], [55], [56], [57], [58], [59], IR-UWB [60], FMCW [61], [62], and microwave [63], [64] sensors.

When comparing the known parameters of the sensors, key differences and commonalities are evident. The operating frequencies of available UWB sensors [55], [56], [57], [58], [60] lie in the range of 3-9 GHz and are consistently lower than FMCW sensors operating frequencies [61], [62]. The highest center frequency goes up to 9 GHz for UWB radars. In contrast, the FMCW sensors carry a center frequency greater than 20 GHz. Additionally, the bandwidth of UWB radar sensors is quite large (0.55 GHz [56] to 6.3 GHz [59]) as compared to microwave [63], [64], and FMCW radar sensors [61], [62]. This characteristic sets UWB radars apart from other sensors as it facilitates their ability to permeate through walls, along with other conventional applications to detect, track, and recognize targets through walls [53], [54], [57], [59], [60]. In retrospect, the microwave and FMCW sensors offer the same capabilities but are not suitable for TTW applications.

In terms of detection range, Pulseone 410 [58] offers the highest 400 m detection range for target tracking, while Position2Go [62] can serve the same purpose for up to 12 m range. For human presence detection, sensors based on UWB, IR-UWB, microwave, and FMCW radar technology, HST-S1M-SE [55], SLMX4 [60], SEN0192 [63], and Position2Go [62] can work up to 13.4 m, 10 m, 16 m, and 12 m, respectively. It is important to keep in mind the operating conditions and available interfacing options for connecting processing units of these sensors while making selections for their potential applications.

IV. HUMAN ACTIVITY RECOGNITION AND VITAL SIGNS CHARACTERIZATION USING UWB RADAR TECHNOLOGY AND MACHINE LEARNING

The emergence of machine learning has prompted researchers to utilize its capabilities in further enhancing the capabilities of UWB radar systems for numerous applications. Systems are designed to automatically detect and

TABLE 6. Systematic critical comparison of reviewed commercially available radar sensor.

Architecture	Datasheet	Radar Sensor	Center Frequency	Bandwidth	Beamwidth	Detection Range (no wall)	Potential Applications
UWB	[53]	LT105 OEM	—	7.3-8.5 GHz	30°azimuth 120°azimuth	10 m	Respiration Presence detection Gesture recognition
	[54]	LT103 OEM-xG	—	7.3-8.5 GHz	±60°azimuth ±60°elevation	10 m	Respiration Position tracking Presence detection Gesture recognition
	[55]	HST-S1M-SE	3-4.0 GHz	0.45-1 GHz	—	13.4 m	Vital Signs Presence detection
	[56]	SR-RUG0-083M-01	7-9 GHz	0.5-1.4 GHz	—	4 m	People counting Motion detection Collision avoidance Presence detection
	[57]	Radarbolaget	2 GHz	0.5-2.5 GHz	—	20 m	Through wall measurement Material investigation
	[58]	PulseOn 410	3-5 GHz	1.4 GHz (RF BW)	—	400 m	Target tracking
	[59]	Walabot	—	3.3-10 GHz	—	10 m	In-room & in-wall imaging Object detection & tracking Motion sensing
IR-UWB	[60]	SLMX4	7.29 GHz	6.13-10.76 GHz	—	10 m	Presence detection Respiration Target distance
Microwave	[63]	SEN0192	—		72°azimuth 36°pitch	16 m	Motion detection
	[64]	XYC-WB-DC	5.8 GHz	—	—	9 m	Auto-sensing Automation
FMCW	[61]	LD2410	24 GHz	—	—	6 m	Respiration Presence detection
	[62]	Position2Go	25 GHz		76°azimuth	12 m	Target tracking

configure the number of people present behind a wall, track their actions, and assess what movements are being performed [20], [25], [26], [32], [36]. By using artificial intelligence (AI) automated solutions, the operator can securely determine the status of an unknown environment at a safe distance.

The following section is divided into different segments organized based on the state of the target. Human motion indicates when a human target location is dynamically changing in an environment. The human presence discusses studies for stationary targets. The following section includes the extraction of vital signs and overall applications related to the healthcare sector. The researchers have implemented the benefits of UWB radars by detecting non-human targets such as drone detection and localization [35], soil moisture, obstacle, and traffic detection [22], [23], [33], [34], [69], [70]. A series of experimental settings identifying four different target classes have been demonstrated in Figure 12.

Convolutional neural network (CNN), a type of deep neural network (DNN) has various applications related to computer vision and image analysis [35], [102], [103], [104] and has also been extensively used for human activity recognition based on pre-processed radar signals. They are made up of multiple layers, including the input layer, the convolutional layer, the fusion layer, the dense layer, and the output layer, as shown in Figure 11. The input layer functions to provide input to the model. The number of neurons in this layer will be equal to the total number of features in the data. As for the convolutional layer, it is used to extract features by applying filters to the input data. Moreover, the pooling layer is utilized to downsample the data which enhances the efficiency and reduces computation time [102]. Furthermore, the dense layer takes the output of the previous layers and connects their neurons to every neuron in the dense layer. The final layer is the output layer

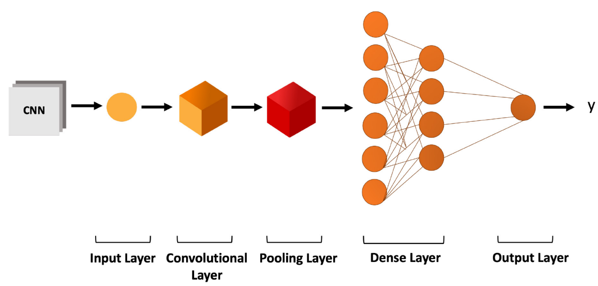

FIGURE 11. A typical architecture of convolutional neural network (CNN).

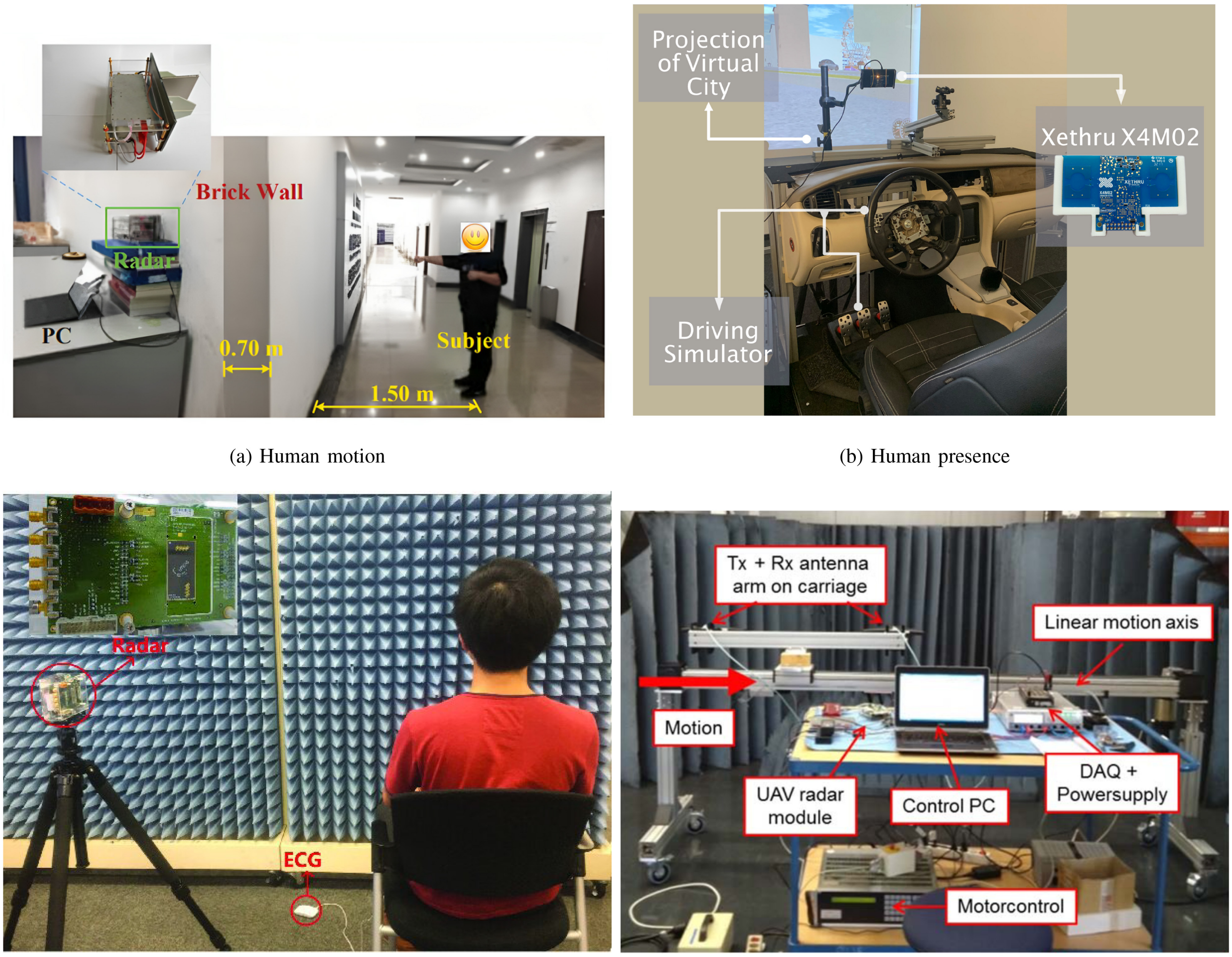

(a) Human motion

(b) Human presence

(c) Vital signs

(d) Non-human

FIGURE 12. (a) The experimental scenario for dataset acquisition with a self-developed TWR [36]; (b) The driving simulator setup used for data collection [48]; (c) Experimental environment: The radar is placed on the left side of the participant. The distance between the radar and the shoulder of the participant is 1.1 m [30]; (d) SAR measurement setup with provisional MW absorber arrangement for trihedral corner reflector (12 cm and 10 cm edge length) as reference targets [86].

that is responsible for producing the network's predictions based on the extracted features.

Unlike conventional shallow algorithms, DNN consists of a higher number of processing layers that are trained to learn complex characteristics of data as it does not rely on manual feature extraction [105]. Although this has advanced the progression of machine learning, DNN algorithms face the challenge of premature convergence and overfitting [102], [103]. Convergence occurs when the weights and biases of the algorithm satisfy the local features while neglecting the global minima of the multidimensional space. This behavior is not favored as it fails to reconcile with characteristics that have not yet been trained upon. On the other hand, overfitting is a common challenge faced by DNN algorithms where results become biased towards the trained data and fail to meet satisfactory results for the testing data [35], [104]. Such behavior indicates that the algorithm has not comprehensively associated certain features with their respective behaviors, and instead has "memorized" their occurrence.

The following section is divided into different segments organized based on the state of the target. Human motion indicates when a human target location is dynamically changing in an environment. The human presence discusses different studies for stationary targets. Next, studies on the extraction of vital signs for a stationary human using AI techniques are reviewed. Lastly, the characterization of non-human objects using radar technology is discussed.

1) HUMAN MOTION

The recognition of human activity with its movement involves the precise analysis of returned UWB radar signal signature features for various motions. These backscattered radar signatures are processed using different machine learning algorithms for the prediction of correct human activity as depicted in Table 7.

The authors [25], [26], [36] employed the UWB radar sensors for the real-time robust classification of dynamic human movements using deep neural networks (DNN), convolution, and auto-encoders. The classification precision

TABLE 7. Comparison of reviewed studies for monitoring human motion and activity using machine learning algorithm and radar technologies.

Class	Ref	Year	Machine Learning		Input	Dataset Size	Accuracy	Real-time Implementation
Human Motion	[25]	2022	CNN		Images	1728 (training) 432 (validation)	97.69% (training) 91.44% (validation)	Yes
	[36]	2020	Neural network	AEN	Signals	864	93%	Yes
				GRU				
	[26]	2022	Multilink auto-encoding neural network	SVD module	Images	≈1740 (training) 432 (validation)		Yes
				Coordinate attention			93.06%	
				LISTA			89.81%	
				Adaptive weight				
	[37]	2016	Squared prediction error		Signals	500 samples (no motion) 7000 samples (motion)	—	Yes
	[38]	2012	—		—			Yes
	[32]	2023	Transformer (3D-TransPOSE)		Signals	105,400 frames (training) 30,750 frames (testing)	—	Yes
	[20]	2021	CNN		Signals	2592 (training) 864 (validation) 864 (testing)	99.7%	No
	[44]	2022	RPCNet	CNN	Signals	—		Yes
				RNN				
	[47]	2021	RNN	EDA	Signals	65,000 samples	99.6%	Yes
				LSTM				
	[46]	2020	KNN		Signals	70 (10 times per movement)	99%	Yes
	[45]	2023	Random forest classifier		Signals	720 samples	93.80%	No
			DL (ResNet50, DenseNet121, LSTM, Transformer)				71.30%	

is determined based on the accuracy of the machine learning structure employed. The algorithm in [25], [26] extracts the frequency domain features of the radar signal initially transmitted from a sensor with a frequency range of 0.5–2.5 GHz. The environmental conditions of the three studies were carried out for targets placed behind a brick wall at 0.23 m [25], [26] and 0.70 m [36]. Following the pre-processing of the acquired data, the input data as signals [36] and images [25], [26] is fed to the machine learning classifier. The studies aim to understand the effectiveness of the algorithm in identifying the movements taking place behind the wall whilst ensuring that the received signals are filtered from noise. The success of the model built by [25] is assessed by decreasing the model's parameters while achieving high recognition rates and real-time recognition. The detection algorithm in [36] experienced minute delays in its recognition rate, which is considered tolerable as it is a function of the target's complexity. Furthermore, because of the gated memory technique used, the model can instantly determine the executed movement. This provides an advantage over other neural networks because conclusions can be reached without requiring the entire movement to be completed. The proposed algorithm yielded an accuracy rate of 97.69% [25], 93% [36], and 93.06% [26] respectively.

A residual subspace projection topology algorithm is proposed in [37] for behind-the-wall recognition of single and multiple people. A total of 7500 samples of backscattered UWB radar signals were taken behind a 23.5 cm brick wall at various positions (no person, one person, and two persons). The compressed detection approach was used to compute the mean squared error (MSE) from the acquired signal dataset. The results showed that the MSE was lowest with no person, followed by one target, then two behind the wall. 3D TransPOSE is a motion detection algorithm used in [32]. The suggested algorithm is based on a transformer architecture. The idea is to use 3D imaging to detect movement behind a 4.5-meter plywood wall. The dataset had 105,400 training frames and 30,750 testing frames and was analyzed using the average precision and percentage of accurate key points. The authors in [46] [45] conducted their research with no wall averting the human target. Hämäläinen et al. [46] based their research on a UWB radar sensor operating at a frequency range of 3.1–4.8 GHz and used a k-nearest neighbor (KNN) technique. Seven motions within the radar's range were performed for ten iterations each. The effectiveness of the implemented model was determined by its skewness and received power. The proposed system achieved 99% accuracy while running in real-time. Using two UWB radars, [45] tested DNN and random forest classifier systems for detecting human movements. The data was collected for 720 samples within range of the radar. The random forest classifier achieved 93.8% accuracy, whereas the DNN system achieved 71.3%.

The Xethru X4M03 UWB impulse radar was used in [84] to classify 14 hand gestures detected by unique feature extraction with the help of CNN. The researchers suggested four distinct classifiers to compare their overall performance in discriminating gestures: fully convolutional neural network (FCNN - network I), k-nearest neighbors (KNN - network II), support vector machine (SVM - network III), and long short-term memory networks (LSTM -network IV). With 250 samples per gesture, 80% are used for training with 5-fold cross-validation, and the remaining samples are used for testing without the training procedure.

According to the results, network IV had the best classification performance and computational cost, with an accuracy of 96.15%. The accuracies of networks III, I, and II were 94.08%, 93.33%, and 92.02%, respectively. The combination of a 2D-CNN with an LSTM model allows for the analysis of time-series inputs and is composed of state/memory cells for storing state/time data. The 2D-CNN collects features in this structure, while the LSTM network establishes the temporal relationship between the features.

The stacked-LSTM, CNN-LSTM, and residual neural network (ResNet) with UWB data gathered using three radars was investigated by [85] for the predictions of numerous human motions. The stacked LSTM-RNN model differs from a single layer in that it can extract richer features. However, this can only be accomplished with a large set of data for training. The CNN-LSTM combination is obtained by adding two LSTM layers to the CNN model and dividing it into five subsequences of 150 samples each. The ResNET architecture is a modern neural network used for function approximation. The dataset used to train each network was made up of several daily human activities. The CNN-LSTM combo outperformed the other models in terms of accuracy, with a success rate of 94%. The classification accuracy of the stacked-LSTM network was only 50%, whereas ResNET obtained 75% accuracy. The authors in [85] discovered that the stacked-LSTM was ineffective in extracting time series features, whereas ResNET was unable to model the temporal components. The CNN-LSTM network, on the other hand, was able to take the efficient features of both models and effectively discriminate between features while modeling temporal components in time series. Its accuracy rate can also be attributed to the model's ability to reduce noise while extracting features and learning temporal relationships.

The recurrent neural network (RNN) architecture differs from CNN in that it focuses on obtaining data in the temporal domain. The RNN algorithm operates in a cycle that utilizes the output of a layer as an input to the subsequent layer. This structure has shown exemplary results for sequential data, where a series of data holds beneficial information for the next set of information [106]. While useful for some applications, its operation is limited by the convolutional filter's window size. That is, neighboring members of the input are fed the same functions, whereas the outputs of distinct functions are processed by filters with different parameters [107]. This method employs a sequential multiplicative process in which the completion of one operation is dependent on the preceding output and is continued until the temporal information can be extracted. As a result, the network is vulnerable to exploding and disappearing gradient issues [108], [109]. To avoid this drawback, researchers have favored the use of the long short-term memory (LSTM) network, a subset of RNN. The network contains cells embedded with self-loops and gating units for memorizing arbitrary time intervals and forgetting inconsequential values or when the output value is required [107]. Furthermore, recent researchers [47], [84], [85] have favored the merging of LSTM with neural networks for the simultaneous processing of sequential and spatial data, respectively.

2) HUMAN PRESENCE

The integration of AI-powered classifiers for the detection of human presence based on radar-backscattered signatures has become popular in recent times as shown in Table 8.

Researchers [41], [48], [50], [51], [52] have developed automated UWB-based systems for the detection of human presence. The study conducted by [52] presents an approach to suppress ghost targets using an FMCW-based radar system. Ghost targets are erroneous detection by the radar system when no person is present. To mitigate their effects and occurrence, the characteristics of the reflected signals are assessed. Taking features such as distance, velocity, azimuth, and elevation angles into account may aid in detecting real targets. The machine learning algorithm is designed based on a DNN classifier. The efficacy of the algorithm is determined based on its ability to suppress ghost targets. Both real and false targets were differentiated with an accuracy of 94.45%.

To identify whether a target is present behind a wall, [51] developed a stepped-frequency continuous-wave (SFCW) radar system for TTW detection. The CNN network allowed for the classification of three classes - no person, standing and sitting. Scenes where a person was occupying the room were assessed from a distance of 2.5 and 5 m away from the wall. Using the inverse Fourier transform, the data was translated from the frequency domain to the spatial domain and categorized using a CNN. For the training and testing phases, a total of 7200 and 1800 samples were accumulated, respectively. For improved differentiation between classes, authors suggested an increase in SFCW frequencies, thus resulting in a larger data set. The developed CNN model produced an accuracy rate of 97%.

Like [51], Hu et al. [50] used extracted data from the UWB multiple-input-multiple-output (MIMO) SFCW

TABLE 8. Comparison of reviewed studies for human presence detection using machine learning algorithm and radar technologies.

Class	Ref	Year	Machine Learning	Input	Dataset Size	Accuracy	Real-time Implementation
Human Presence	[41]	2022	SVM	Signals	—		Yes
			MLP				
			CNN				
	[43]	2016	—				Yes
	[48]	2023	LSTM	Signals	10406 samples	67.20%	No
	[51]	2019	CNN	Images	7200 training 1800 testing	97%	Yes
	[52]	2022	DNN	Signals	120 frames	94.45%	No
	[65]	2022	DL	3D points	120000 frames	—	Yes
	[66]	2021	DNN	Images	4386 frames	98%	No
	[67]	2022	CNN	Signals	36326 samples	—	Yes
	[68]	2020	CNN	Signals	5000 samples	98.3%	No

radar system to detect the presence of a human and their location. To suppress artifacts in the focused image as well as reduce the computing complexity, a cross-correlation-based time domain back projection (CC-TDBP) method is implemented. Three experiments were designed for the testing of the developed MIMO radar and the results are shown in Figure 13. The first test used two dihedral corner reflectors that were approximately about 3 m and 5 m away from the equivalent phase center of the radar system. In the second experiment, two humans acted as targets at a close range. Results showed that humans can be detected in an outside environment. In the last experiment, two humans were standing behind a brick and concrete wall (22.5 cm) with the radar placed 15 cm away from the wall. The results of this experiment showed that when the CC-TDBP algorithm was implemented with the addition of background subtraction, the results were more accurate. By utilizing UWB MIMO radar and DL, Song et al. [65] were able to reconstruct TTW target poses. While the self-developed DL model was computationally operational concerning the compared models, their reconstruction performance was relatively weaker. This is largely attributed to the discrete sampling when converting the 3D images to points, leading to the loss of information. Additionally, the findings of the study suggested that while the decrease in SNR due to the occlusion of the wall is inevitable, the quality of reconstruction and imaging is further abridged.

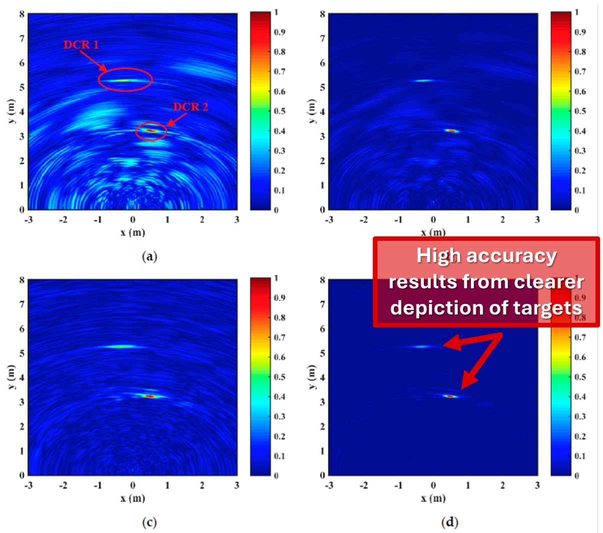

FIGURE 13. Imaging results of two corner reflectors by: (a) the TDBP algorithm with direct coupling removal; (b) the CC-TDBP algorithm with direct coupling removal; (c) the TDBP algorithm with background removal; (d) the CC-TDBP algorithm with background removal [50].

The studies of [65], [66] examined the concept of pose estimation and reconstruction by applying machine learning methods for UWB-based radar data. Human pose estimation (HPE) provides geometric and motion information by estimating the configuration of body parts from data attained by sensors [110]. Determining HPE has recently been accomplished via deep learning (DL) solutions that have outperformed methods such as computer vision. This is usually accomplished through optical cameras that allow the identification of certain features such as position and shape by cultivating an in-depth map. While developed systems have shown exemplary results, the extraction of 3D HPE has been challenging due to depth ambiguity. Additionally, conventional approaches are not liable under obscured environments with harsh lighting or through walls. Aiming to counteract such restrictions, the use of radar sensors working on the micro-Doppler effect has been employed as the extraction of target information regardless of adverse environmental conditions is viable. Xu et al. [66] achieved HPE through backward projection imaging and random forest DNN for feature extraction. The random forest framework consists of decision tree classification models that work in tandem for the best classification at

TABLE 9. Comparison of reviewed legacy studies for healthcare applications using UWB radar technologies and machine learning.

Class	Ref	Year	Machine Learning	Input	Dataset Size	Accuracy	Real-time Implementation
Vital Signs	[30]	2019	CNN	Signals	50000 (training) 25000 (testing)	—	Yes
	[31]	2019	1D-CNN	Signals	1200 datasets	95.9%	No
	[27]	2019	SVM	Signals	15360000 samples	98.7%	Yes
	[28]	2015	WiTrack2.0: Multi-shift FMCW	Signals	5000 location readings per person	—	Yes
			WiTrack2.0: Successive Silhouette Cancellation				
	[29]	2016	CNN	Signals	—	91.31%	No
	[8]	2022	CNN-LSTM	Signals	7000 samples	97%	Yes
	[9]	2022	CNN	Signals	8400 samples	97.53%	Yes
			SVD-EEMD			—	
	[10]	2021	ResNet	Images	230 spectrograms	90%	No
	[11]	2022	CNN-SVM	Images	2500 images	97.4%	Yes

every level. These kinds of ML models are effective for nonlinear data with large datasets. However, decision trees are commonly susceptible to cases of over-fitting, leading to generalized accuracy that is determined based on common predictions [111].

Most of the compared research studies of determining human motion and presence [43], [48], [51], [52], [65], [66], [67], [68] have focused on finding a single target. Table 8 compares the findings of these studies. Under practical circumstances, this would rarely be the case as several people must be identified simultaneously to reduce the number of fatalities in search-and-rescue missions for instance. The study proposed by [67] identifies a solution to this niche problem by devising a method to extract stationary human data TTW. In addition to the use of an IR-UWB radar, a six-layered CNN algorithm is employed in addition to the target point of interest (TPOI) for the detection of multiple targets. Researchers noted that their proposed algorithm has a 3% false alarm rate. The effectiveness of the model was compared with three other methods that ranged between a 35-65 percentile rate of missed alarms. The algorithm used by [67] had the tabulated rate at a range of 6 cm, while the other three models ranged between 15 cm to 17 cm. This appears to be an unfair comparison as the other models were compared at a distant range while the researchers in [67] opted to assess the results at a relatively closer range.

3) HUMAN PRESENCE & VITAL SIGNS

Besides only human motion and presence detection in [20], [26], [36], [37], [43], [44], [46], [48], [51], [52], [65], [66], [67], [68], many studies have been reported to monitor the vital signs of the target along with its detection. Table 9 presents a comprehensive comparison of such studies.

The authors in [27], [28], [42] employed a UWB radar to identify human movement and monitor vital signs with the help of machine learning. Wu et al. [30] employed a MIMO UWB radar to identify people and estimate their heart rates. The 75,000 samples acquired from the MIMO UWB radar was transformed into a 2D matrix for feeding to the CNN classifier. The 50,000 samples were used for training and 25,000 were used for testing. The study by [27] used four data sets to develop an efficient machine-learning model for the prediction of human presence, movement, and vital signs. The study conducted three experiments: no one in the sight of the radar, vital signs being measured, and the target subject moving. The three tests were labeled 0 through 2 accordingly, while the fourth and final test were a composite of the first three. The SVM was used to classify the 15,360,000 data, providing a prediction accuracy rate of 98.7%. While effective, the use of SVM poses certain limitations in the accurate determination of breathing rates. According to [31], algorithms such as SVM lack in robustness when classifying and recognizing the rates of eupnea and bradypnea. On the contrary, the 1D-CNN algorithm proposed by [31] was able to effectively recognize the four human respiration rates - eupnea, bradypnea, tachypnea, and apnea.

The self-developed multi-shift FMCW radar operating at a frequency range of 5.5-7.2 GHz was tested with the proposed WiTrack2.0 algorithm in [28]. Each test for the proposed method contained 100 experiments that were evenly divided between the line of sight and TTW (15.24 cm). Results showed that WiTrack2.0 can track up to five users with improved precision in line-of-sight settings at a range of 10 m. When assessing the ability of the system to detect vital signs, the breathing rate performed better for static users than for moving users. While the reported system is robust to simultaneously track multiple users, it was not able to precisely determine the location of each.

Researchers have employed CNN-based algorithms due to their aptitude for classifying non-linear behaviors in UWB radar datasets. This proficiency has greatly benefited the use of UWB sensors for the extraction of physiological signals such as heart rate (HR) [30]. The healthcare sector has been disrupted by the benefits of UWB radars over traditional devices such as electrocardiogram (ECG) monitoring devices. In addition to the benefits offered by UWB radar sensors, their compactness and power efficiency have been integrated as biosensors in healthcare applications [83]. This feature has prompted researchers to explore their integration in diverse applications, such as fetal monitoring [17], [71], [74], [75].

The authors in [29], [30], [31] focus on the extraction of vital signs using a simple CNN model. Wu et al. proposed an HR estimation system to determine the heartbeat of a specific user. The CNN algorithm is trained using a dataset of 50000 samples were acquired using a MIMO UWB radar. The output waveform acquired by the radar must reflect the ECG waveform for the computation of the HR for effective training. However, researchers faced a challenge because the RST intervals of the predicted ECG waveform were sharper in behavior than regular radar waveforms. Researchers have utilized two triangular waveforms to represent the R and S waves instead of the original ECG waveform for the training process to mitigate the RST problem. However, this raised some concerns as changing the shape or representation of ECG waveforms may omit critical information that may be threatening if lost in translation as key characteristics may be altered.

The CNN model devised by researchers in [29] has a cascade structure designed to capture both ECG and heartbeat signals for improved classification outcomes. ECG recordings inherently carry the bio-electrical features of heartbeats, while radar data provides the physical characteristics such as amplitude and the intervals between beats. By recognizing this, researchers designed two isolated one-dimensional (ID)-CNNs in cascade to analyze the ECG and heartbeat signals. This is then followed by another CNN integrated to understand the observed features of the signals. These isolated modules are then integrated, thus combining the strengths of both signal types for improved accuracy. Overall, this approach demonstrates the importance of tailoring certain algorithmic structures for specific classification tasks.

Compared to the approaches mentioned above that were based solely on CNN classifiers, the authors [8], [9], [11] used more sophisticated algorithms that combined the benefits of CNN with the features of other models. The detection and localization of breast cancer were investigated in [8] by utilizing a CNN and long short-term memory (LSTM) algorithm. Diagnostic methods have traditionally taken place through mammography X-ray and magnetic resonance imaging (MRI) that bring forth disadvantages such as their cost, size, and radiation. UWB radars have been investigated as an alternative method that can differentiate the dielectric properties of cancer tissues from normal breast tissues in the microwave frequency band [112], [113].

$$\varepsilon_{br}(\omega) = \varepsilon_\infty + \frac{\varepsilon_s - \varepsilon_\infty}{1 + j\omega\tau} + \frac{\sigma_s}{j\omega\varepsilon_0} \tag{3}$$

In the one-pole Debye Equation (3) [113], ω is the frequency, whereas the dielectric constants ε_s, ε_∞, and ε_0 represent the low, high, and free-space frequencies, respectively. While determining the dielectric property of the internal structure has been proven to be complex, its extraction has been simplified with the integration of machine learning methods. The majority of emerging research has focused solely on detecting tumors via machine learning while disregarding their location, rendering them impractical in realistic applications.

The research by [8] aims to simultaneously perform both tasks through the addition of the LSTM structure. Employing the CNN algorithm aims to extract distinct features, which are then used as input to the LSTM network to process the time series data. As a result, the LSTM network analyzes the time-domain backscattered signal and learns the time-of-arrival (ToA) of the tumor response. The dataset utilized for the training of the proposed algorithm was accumulated using the breast phantoms and detection experimental system conveyed in [8]. This demonstrated that an architecture with two CNN layers and a singular LSTM layer retrieved optimal results with an accuracy of 100%, 99.56%, and 89.50% for training, validation, and testing, respectively.

4) NON-HUMAN TARGETS

The use of UWB radar technology for the detection and characterization of non-human objects is well investigated too. Researchers [33], [34] have expanded the application of UWB radars for the identification of non-human targets. A comparison of reviewed relevant studies is given in Table 10. Kawaguchi et al. [33] concentrated on drone categorization utilizing deep learning and UWB radar image recognition [35]. The radar data was preprocessed using a CNN-based model while images served as the input of AlexNet CNN model. The accumulated data consisted of 300 frames originating from 50 frames of radar images per target. The 60% of the data was used for training, while the remaining 40% was used for testing. The algorithm's ability to distinguish between targets was assessed using two scenarios: one frame of a radar image as input and two consecutive frames of a radar image as input. Because the radar echoes' temporal variations were taken into account when calculating the feature amounts in the second case, the results showed greater accuracy levels at approximately 90%.

Using both a simple pattern recognition algorithm (KNN) and a deep convolutional neural network (CNN), the study [34] managed to reconstruct unknown targets behind a 0.15 m thick wall. By recording the electric field profile at multiple points using multiple receivers, a time series of data is obtained which will be used as the data for target reconstruction and classification. The 2D-time series data was converted to a 2D array before feeding to the CNN classifier. The experimental results showed that the KNN algorithm sufficiently approximated the location of simple circular objects at a fixed location and radius with an accuracy of 97%. However, the CNN via Keras-TensorFlow produced impressive results after adequate training with an accuracy

TABLE 10. Comparison of reviewed legacy studies for detection and characterization of the non-Human targets healthcare using UWB radar technologies and machine learning.

Class	Ref	Year	Machine Learning	Input	Dataset Size	Accuracy	Real-time Implementation
Non-Human	[33]	2021	AlexNet (CNN)	Images	300 frames	—	Yes
	[34]	2020	CNN	Signals	10000 samples	99%	Yes
			KNN			97%	
	[22]	2022	Shallow Neural Network	Signals	—	98.94%	No
	[23]	2023	DNN	Signals	1000 data instances	—	No
	[69]	2021	RNN-LSTM	Signals	47000 signals	81%	No
	[70]	2022	Statistical method	Signals	—	96%-98%	Yes

of >99% even with complex objects. The total number of samples for this experiment was 10,000 and this experiment proved it is more accurate and less time-consuming.

The use of neural networks is investigated by researchers [22], [23] for the identification of soil moisture. This niche application allows for the surveillance of vegetation and crops in the agricultural sector. The study [22] utilizes the Walabot UWB radar sensor to determine the dielectric constant of soil. The signals reflected from the soil samples are preprocessed and utilized as input to the proposed model. The investigated models included KNN, SVM, and linear regression. Researchers noted that the linear regression outperformed the aforementioned models. However, with the introduction of a neural network algorithm, the data was classified with higher accuracy results. While results showed high portal-time or real-time employability, researchers limited their research by investigating one type of soil instead of expanding the success of their results across different soil types and compositions. Ding et al. [23] proposed SoilId - a soil moisture unmanned aerial vehicle (UAV) sensing system equipped with an IR-UWB sensor. The deep neural network was fed 1000 data instances from the collected data signals. The UWB-mounted UAV system requires less than two minutes to measure the moisture of the soil. While this is relatively quick, it may cause time implications for farms that have large land acreage.

The researchers [70] proposed a solution intended for use in the transportation industry by devising a portable device for traffic counting and speed estimation. The detection and counting of vehicles is satisfied using statistical and signal processing techniques. This entails the use of peaks and trajectories for the localization of the counted vehicles on the surveyed road. The real-time testing took place to verify the validity of the proposed system, resulting in an accuracy of 96% for larger vehicles and 98% for smaller vehicles.

V. DISCUSSION

In terms of the preferred UWB architecture, IR-UWB sensors serve a wider range of applications as their signals are rapidly transmitted over a wide spectrum. This enhances its ability to penetrate through obstacles effectively. Most of the surveyed research [27], [32], [44], [45], [47], [48], [70], [84] employing IR-UWB sensors relied on the Novelda XeThru sensor range. Additionally, the hardware implementation of UWB-based radar devices are significantly more compact than other systems. This further demonstrates the practical applicability of UWB radar across various sectors. Unlike conventional TTW radar systems, which often require multiple large-scale antennas, UWB radar systems are typically transceivers with miniature Tx-Rx antennas. In terms of radar hardware, successful TTW detection is achievable when the antenna has a sufficient coupling ability with the wall, ensuring maximum power transmission through walls while minimizing refractions [114]. For improved range resolution, additional antennas can integrated with UWB radars without compromising the overall size of the device. Consequently, the system's SNR is improved and with further processing methods, the interference of environmental noise is reduced for optimal extraction, optimization, and imaging of radar data.

When combined with signal processing and machine learning approaches for robust systems, UWB radar technology has the potential to revolutionize an array of industries. In this research, different signal processing techniques were used to determine the optimal approaches for achieving high accuracy and reliability. Many academics have worked on the ability to reduce noise and improve the quality of UWB signals under real-world conditions. The signal attenuation advancements lead to reliable solutions for the diverse uses of UWB technology. Recent developments have centered on the usage of device-free monitoring systems. This has been a transformative breakthrough that eliminates the need for invasive gadgets and paves the path for practical solutions that can comfortably service a broader range of needs. Despite the successes, challenges such as multiple people tracking, identification, and vital signs monitoring of moving individuals are evident. The incorporation of machine learning algorithms such as CNN has targeted and aided in the resolution of the aforementioned difficulties. Their combination with UWB radar technology has resulted in considerable advances in person detection, vital sign monitoring, and object recognition.

The use of machine-learning learning models has emerged as the preferred choice of researchers for the characterization of human and non-human targets. Among various machine learning algorithms, CNN models have been viewed as the preferred approach for real-time detection and vital sign analysis [20], [25], [33], [51]. The studies based on CNN algorithms have witnessed an increased training accuracy as exhibited in [20], [25], [33], [51]. Additionally, while signal processing has been widely discussed and showed major improvements in the algorithm, its processing is a computational burden. Instead, CNN has been widely used by researchers [32], [73] as a feature extractor that eliminates the need for the manual processing of UWB data. Its success prompted the integration of CNN architecture with the use of LSTM. This combination has been discussed in [47], [84], [85] to further enhance the performance of the classifier network. CNN serves to extract common features exhibited in the data, while LSTM simultaneously works to identify the temporal relationships. Continued research in this area intends to address difficulties and improve the accuracy and dependability of UWB-based systems in real-world scenarios, reinforcing its role in improving healthcare, security, and emergency response operations.

VI. FUTURE RESEARCH TRENDS

As radar techniques continue to advance, several key factors are going to influence the future of through-the-wall human activity recognition. A key focus is on increasing the use of UWB radar, which exhibits exceptional spatial resolution and the ability to capture the smallest movement of humans behind the wall [67]. UWB are known for their wide frequency range, allowing them to detect subtle motions more accurately and improve their penetration through various materials such as drywall and wood. This advancement would facilitate more precise and reliable recognition of humans in complex environments, establishing UWB radars as a major pillar of future research in this field.

Complementing UWB radars, simpler radar techniques such as millimeter-wave (mmWave) radars can also be used. Although these types of radar offer high resolution, their penetration capabilities are not as effective compared to UWB radars, since the density of the obstacle can affect the signal, making it less sensitive to subtle human movements. However, they are still suitable for TTW human detection if the material density is not an issue [115], [116], [117]. The aforementioned radar technologies can be further enhanced by integrating machine learning and deep learning techniques, which are expected to transform data interpretation. These methods can improve accuracy, enable transfer learning, and reduce false positives, facilitating real-time processing that has been employed by [67], [115], [116], [117]. Furthermore, [117] also discussed the miniaturization of radar systems, specifically the antenna, and efforts to make them more compact hold significant potential for enhancing performance, reducing costs, and expanding their applications making these technologies more accessible for consumer applications.

While radar-based techniques are leading the way, nonradar-based techniques such as computer vision and thermal imaging can also be used in through-the-wall human activity recognition as discussed in [118], [119], [120]. These techniques often rely on visual data and temperature variations to detect and classify movements. Although they may be effective in some scenarios, issues like obstacles, lighting conditions, and privacy concerns that were discussed in [121], can significantly limit their effectiveness. Radar-based techniques, specifically UWB and mmWave radars, provide notable advantages over non-radar techniques. They provide superior penetration through obstacles and can operate in harsh environmental conditions for instance, during a fire, where thermal-based might fail. Moreover, radar technologies are considered less abusive, as they maintain the privacy of individuals by not capturing detailed visual images. In contrast, non-radar techniques like computer vision, can offer higher accuracy detecting humans when they are in line-of-sight and that accuracy decreases immensely when the target is obscured. To maximize the benefits of both radar and non-radar technologies, multi-modal fusion was utilized in [122], [123]. The integration of various types of sensors created a more comprehensive and robust system for activity recognition. This combined approach can overcome the limitations of individual sensors, leading to more accurate recognition and reliable capabilities.

In conclusion, combining advanced radar techniques, machine learning, and multi-modal fusion is expected to yield significant results in through-the-wall human activity recognition, leading to systems that are more effective, responsive, and adaptable to various environments.

VII. CONCLUSION

This study has thoroughly explored the intricate principles of UWB radar architectures, processing methods, and their effectiveness in numerous real-world applications. The utilization of UWB radar systems is continuously growing and is being explored in areas beyond search and rescue missions, making breakthroughs in the medical industry. The processing methods of UWB signals were analyzed and compared for a concise understanding of what is best fit for the characteristics of UWB signals. The surveyed research for the extraction of vital signs relies on detecting breathing and heartbeat patterns based on their corresponding frequency windows. Determining human presence and mobility varies from study to study. The unified goal, however, is to decrease noise and enhance regions where a target and its related movement have high density. This detailed review has proved that the integration of machine learning algorithms, especially CNN, with UWB radar technology, has enhanced the classification accuracy of human activity as well as vital signs characterization. With additional research and development, we can expect even more innovative applications and enhanced techniques, which will solidify UWB radar's position as a fundamental radar technology in different industries. Whether it's strengthening security, or enhancing automated robot systems, UWB radar technology proves its innovative capabilities in addressing complex challenges and making the world safer.

REFERENCES

[1] H.-S. Cho and Y.-J. Park, "Classification of human body motions using an ultra-wideband pulse radar," *Technol. Health Care*, vol. 30, no. 1, pp. 93–104, 2022. [Online]. Available: https://doi.org/10.3233/THC-212827

[2] S. Wang and W. Weng, "Dilemmas and directions of real-time detecting trapped individuals using ultra-wideband radar in building fire rescue," *Frequenz*, vol. 77, nos. 9–10, pp. 425–442, 2023. [Online]. Available: https://doi.org/10.1515/freq-2022-0237

[3] L. Barbieri, M. Brambilla, A. Trabattoni, S. Mervic, and M. Nicoli, "UWB Localization in a smart factory: Augmentation methods and experimental assessment," *IEEE Trans. Instrum. Meas.*, vol. 70, pp. 1–18, 2021.

[4] A. A. Pramudita et al., "Soil water content estimation with the presence of vegetation using ultra wideband radar-drone," *IEEE Access*, vol. 10, pp. 85213–85227, 2022.

[5] R. Prasanna, K. Annaram, and K. Venkatalakshmi, "Framework for touchless patient monitoring system integrating ultra-wideband radar and internet of things for Covid-19 patients," *Int. J. Multiscale Comput. Eng.*, vol. 20, no. 4, pp. 57–69, 2022.

[6] D.-S. Kim and H. Tran-Dang, *Ultra-Wideband Technology for Military Applications*. Cham, Switzerland: Springer, 2019, pp. 197–204. [Online]. Available: https://doi.org/10.1007/978-3-030-04927-0_15

[7] H. A. G. C. Premachandra, R. Liu, C. Yuen, and U.-X. Tan, "UWB radar SLAM: An anchorless approach in vision denied indoor environments," *IEEE Robot. Autom. Lett.*, vol. 8, no. 9, pp. 5299–5306, Sep. 2023.

[8] M. Lu, X. Xiao, Y. Pang, G. Liu, and H. Lu, "Detection and localization of breast cancer using UWB microwave technology and CNN-LSTM framework," *IEEE Trans. Microw. Theory Techn.*, vol. 70, no. 11, pp. 5085–5094, Nov. 2022.

[9] S. Liu et al., "An intelligent signal processing method for motional vital signs detection system based on deep learning," *IEEE Access*, vol. 10, pp. 106463–106481, 2022.

[10] U. Saeed et al., "Portable UWB RADAR sensing system for transforming subtle chest movement into actionable micro-doppler signatures to extract respiratory rate exploiting ResNet algorithm," *IEEE Sensors J.*, vol. 21, no. 20, pp. 23518–23526, Oct. 2021.

[11] F. Khan, S. Azou, R. Youssef, P. Morel, and E. Radoi, "IR-UWB radar-based robust heart rate detection using a deep learning technique intended for vehicular applications," *Electronics*, vol. 11, no. 16, p. 2505, 2022. [Online]. Available: https://www.mdpi.com/2079-9292/11/16/2505

[12] J. C. Bancroft, "Introduction to matched filtering," *Crewes*, vol. 14, pp. 1–8, Jan. 2002.

[13] M. Soori, B. Arezoo, and R. Dastres, "Artificial intelligence, machine learning and deep learning in advanced robotics, a review," *Cogn. Robot.*, vol. 3, pp. 54–70, Apr. 2023.

[14] S. Z. Gurbuz, K. L. Bell, and M. S. Greco, "Integrating AI into radar system design: Next-generation cognitive radars," in *Women in Telecommunications*. Cham, Switzerland: Springer, 2023, pp. 187–222.

[15] F. Berland et al., "Cylindrical MIMO-SAR imaging and associated 3-D fourier processing," *IEEE Open J. Antennas Propag.*, vol. 3, pp. 196–205, 2022.

[16] I. Ahmad, A. S. Hussaini, I. Tamer, A. Amar, J. Rodriguez, and R. Abd-Alhameed, "UWB radar technology," presented at IMDC-IST, Jan. 2022.

[17] E. Arasteh et al., "Unobtrusive cot side sleep stage classification in preterm infants using ultra-wideband radar," *Front. Sleep*, vol. 2, Jun. 2023, Art. no. 1150962. [Online]. Available: https://www.frontiersin.org/articles/10.3389/frsle.2023.1150962

[18] J. Zhang et al., "A multi-target Localization and vital sign detection method using ultra-wide band radar," *Sensors*, vol. 23, no. 13, p. 5779, 2023. [Online]. Available: https://www.mdpi.com/1424-8220/23/13/5779

[19] C. Hadjipanayi et al., "Remote gait analysis using ultra-wideband radar technology based on joint range-doppler-time representation," *IEEE Trans. Biomed. Eng.*, early access, May 3, 2024, doi: 10.1109/TBME.2024.3396650.

[20] Z. Zhengliang, Y. Degui, Z. Junchao, and T. Feng, "Dataset of human motion status using IR-UWB through-wall radar," *J. Syst. Eng. Electron.*, vol. 32, no. 5, pp. 1083–1096, 2021.

[21] J. Peabody, G. L. Charvat, J. Goodwin, and M. Tobias, "Through-wall imaging radar," *Lincoln Lab. J.*, vol. 19, no. 1, pp. 1–11, 2012. [Online]. Available: https://api.semanticscholar.org/CorpusID:41614

[22] A. Uthayakumar, M. P. Mohan, E. H. Khoo, J. Jimeno, M. Y. Siyal, and M. F. Karim, "Machine learning models for enhanced estimation of soil moisture using wideband radar sensor," *Sensors*, vol. 22, no. 15, p. 5810, 2022. [Online]. Available: https://www.mdpi.com/1424-8220/22/15/5810

[23] R. Ding et al., "Soil moisture sensing with UAV-mounted IR-UWB radar and deep learning," *Proc. ACM Interact. Mob. Wearable Ubiquitous Technol.*, vol. 7, no. 1, Mar. 2023, Art. no. 3580867. [Online]. Available: https://doi.org/10.1145/3580867

[24] N. Maaref and P. Millot, "Array-based UWB FMCW through-the-wall radar," in *Proc. IEEE Int. Symp. Antennas Propag.*, 2012, pp. 1–2. [Online]. Available: https://api.semanticscholar.org/CorpusID:30094311

[25] W. Gao, X. Yang, X. Qu, J. Liao, Z. Yin, and D. Zhang, "Indoor human motion recognition method based on kernel-distance doppler velocity estimation and lightweight network," in *Proc. APSIPA ASC*, 2022, pp. 2058–2064.

[26] W. Gao, X. Yang, X. Qu, and T. Lan, "TWR-MCAE: A data augmentation method for through-the-wall radar human motion recognition," *IEEE Trans. Geosci. Remote Sens.*, vol. 60, pp. 1–17, 2022.

[27] Y.-J. Park and H.-S. Cho, "An experiment of human presence and movement using impulse radar and machine learning," in *Proc. Int. Conf. Inf. Commun. Technol. Converg. (ICTC)*, 2019, pp. 12–17.

[28] F. Adib, Z. Kabelac, and D. Katabi, "Multi-person localization via RF body reflections," in *Proc. 12th USENIX Symp. Netw. Syst. Design Implement. (NSDI)*, 2015, pp. 279–292. [Online]. Available: https://www.usenix.org/conference/nsdi15/technical-sessions/presentation/adib

[29] W. Yin, X. Yang, L. Zhang, and E. Oki, "ECG monitoring system integrated with IR-UWB radar based on CNN," *IEEE Access*, vol. 4, pp. 6344–6351, 2016.

[30] S. Wu et al., "Person-specific heart rate estimation with ultra-wideband radar using convolutional neural networks," *IEEE Access*, vol. 7, pp. 168484–168494, 2019.

[31] S.-H. Kim and G.-T. Han, "1D CNN based human respiration pattern recognition using ultra wideband radar," in *Proc. Int. Conf. Artif. Intell. Inf. Commun. (ICAIIC)*, 2019, pp. 411–414.

[32] G. W. Kim, S. W. Lee, H. Y. Son, and K. W. Choi, "A study on 3D human pose estimation using through-wall IR-UWB radar and transformer," *IEEE Access*, vol. 11, pp. 15082–15095, 2023.

[33] D. Kawaguchi, R. Nakamura, and H. Hadama, "Evaluation on a drone classification method using UWB radar image recognition with deep learning," in *Proc. IEEE 93rd Veh. Technol. Conf.*, 2021, pp. 1–5.

[34] A. Wood, R. Wood, and M. Charnley, "Through-the-wall radar detection using machine learning," *Results Appl. Math.*, vol. 7, Aug. 2020, Art. no. 100106.

[35] J. Yousaf et al., "Drone and controller detection and Localization: Trends and challenges," *Appl. Sci.*, vol. 12, no. 24, p. 12612, 2022.

[36] X. Yang, P. Chen, M. Wang, S. Guo, C. Jia, and G. Cui, "Human motion Serialization recognition with through-the-wall radar," *IEEE Access*, vol. 8, pp. 186879–186889, 2020.

[37] W. Wang, D. Wang, and Y. Jiang, "Multiple statuses of through-wall human being detection based on compressed UWB radar data," *EURASIP J. Wireless Commun. Netw.*, vol. 2016, p. 203, Aug. 2016.

[38] J. Li, Z. Zeng, J. Sun, and F. Liu, "Through-wall detection of human being's movement by UWB radar," *IEEE Geosci. Remote Sens. Lett.*, vol. 9, no. 6, pp. 1079–1083, Nov. 2012.

[39] L. Zhao et al., "UWB radar features for distinguishing humans from animals in an actual post-disaster trapped scenario," *IEEE Access*, vol. 9, pp. 154347–154354, 2021.

[40] Z. Yang, J. Cheng, Q. Qi, X. Li, and Y. Wang, "A method of UWB radar vital detection based on P time extraction of strong vital signs," *J. Sens.*, vol. 2021, pp. 1–10, Sep. 2021.

[41] L. Nosrati, M. S. Fazel, and M. Ghavami, "Improving indoor localization using mobile UWB sensor and deep neural networks," *IEEE Access*, vol. 10, pp. 20420–20431, 2022.

[42] A. Kumar, Z. Li, Q. Liang, B. Zhang, and X. Wu, "Experimental study of through-wall human detection using ultra wideband radar sensors," *Measurement*, vol. 47, pp. 869–879, Jan. 2014.

[43] V. Mérelle, A. Gaugue, G. Louis, and M. Ménard, "UWB pulse radar for micro-motion detection," in *Proc. 8th Int. Conf. Ultrawideband Ultrashort Impulse Signals (UWBUSIS)*, 2016, pp. 152–155.

[44] J.-H. Choi, J.-E. Kim, and K.-T. Kim, "Deep learning approach for radar-based people counting," *IEEE Internet Things J.*, vol. 9, no. 10, pp. 7715–7730, May 2022.

[45] D. K.-H. Lai et al., "Dual ultra-wideband (UWB) radar-based sleep posture recognition system: Towards ubiquitous sleep monitoring," *Eng. Regenerat.*, vol. 4, no. 1, pp. 36–43, 2023.

[46] M. Hämäläinen et al., "Ultra-wideband radar-based indoor activity monitoring for elderly care," *Sensors*, vol. 21, no. 9, p. 3158, 2021.

[47] F. M. Noori, M. Z. Uddin, and J. Torresen, "Ultra-wideband radar-based activity recognition using deep learning," *IEEE Access*, vol. 9, pp. 138132–138143, 2021.

[48] I. Brishtel, S. Krauss, M. Chamseddine, J. R. Rambach, and D. Stricker, "Driving activity recognition using UWB radar and deep neural networks," *Sensors*, vol. 23, no. 2, p. 818, 2023. [Online]. Available: https://www.mdpi.com/1424-8220/23/2/818

[49] M. A. Y. Medina, H. J. M. Odiaga, and S. A. Navarro, "Through-wall movement detection based on S-band FMCW radar: An experimental assessment," in *Proc. IEEE MTT-S Latin America Microw. Conf. (LAMC)*, 2018, pp. 1–3.

[50] Z. Hu et al., "Design and analysis of a UWB MIMO radar system with Miniaturized Vivaldi antenna for through-wall imaging," *Remote Sens.*, vol. 11, no. 16, p. 1867, 2019. [Online]. Available: https://www.mdpi.com/20724292/11/16/1867

[51] A. Kılıç, s. Babaoğlu, A. Babalik, and A. Arslan, "Through-wall radar classification of human posture using convolutional neural networks," *Int. J. Antennas Propag.*, vol. 2019, pp. 1–10, Mar. 2019.

[52] T. Jeong and S. Lee, "Ghost target suppression using deep neural network in radar-based indoor environment mapping," *IEEE Sensors J.*, vol. 22, no. 14, pp. 14378–14386, 2022.

[53] *LT105OEM UWB Radar Module*, ARIA Sensing, Rezzato, Italy, Dec. 2020.

[54] *LT103OEM XG Radar Module*, ARIA Sensing, Rezzato, Italy, Oct. 2020.

[55] *User's Manual HST-S1M-CT (for CE/FCC/KC Certification)*, UMAIN, Stockholm, Sweden, 2024.

[56] "UWB RADAR MODULE for short range detection," SR-RUG0-083M-01 Datasheet, Silicon R&D, Seongnam, Republic of Korea, Aug. 2020.

[57] "Radarbolaget." 2024. [Online]. Available: https://www.radarbolaget.com/products/radar-developer-kit

[58] *PulseOn410 Ultra Wideband Radar Module*, Time Domain, Huntsville, Alabama, Aug. 2020. [Online]. Available: https://www.ion.org/gnss/upload/files/904_PulsON%20UWB%20Lab.pdf

[59] *Programmable 3D Imaging Sensor*, Walabot, Yehud-Monosson, Israel, Aug. 2020. [Online]. Available: https://cdn.sparkfun.com/assets/learn_tutorials/7/2/4/walabot-tech-brief-416.pdf

[60] "LMX4 Datasheet," Data Sheet, Sens. Logic, Bozeman, MT, USA, May 2022. [Online]. Available: https://sensorlogic.ai/SLMX4

[61] *Human Presence Radar LD2410*, Robot. BD, Dhaka, Bangladesh, May 2022. [Online]. Available: https://shorturl.at/Rd4dK

[62] "Position2Go development kit." infineon. Dec. 2018. [Online]. Available: https://www.infineon.com/dgdl/Infineon-Position2Go_development_kit-PB-v01_00-EN.pdf?fileId=5546d46267c74c9a0167cabc70cd0120

[63] "SEN0193," 2018. [Online]. Available: https://www.chipdigger.com/pdut/SEN0193/2793949.htm

[64] "XYC-WB-DC-microwave-radar-motion-sensor-module," e Gizmo, 2017. [Online]. Available: https://www.e-gizmo.net/oc/kits%20documents/XYC-WB-DC%20Microwave%20Radar/xyc-wb-dc.pdf

[65] Y. Song, T. Jin, Y. Dai, and X. Zhou, "Efficient through-wall human pose reconstruction using UWB MIMO radar," *IEEE Antennas Wireless Propag. Lett.*, vol. 21, no. 3, pp. 571–575, Mar. 2022.

[66] D. Xu, Y. Liu, and Q. Wang, "Random forest-based human pose detection system for through-the-wall radar," in *Proc. J. Phys. Conf. Ser.*, Jul. 2021, Art. no. 12040.

[67] C. Shi, Z. Zheng, J. Pan, Z.-K. Ni, S. Ye, and G. Fang, "Multiple stationary human targets detection in through-wall UWB radar based on convolutional neural network," *Appl. Sci.*, vol. 12, no. 9, p. 4720, 2022. [Online]. Available: https://www.mdpi.com/2076-3417/12/9/4720

[68] Y. Ma et al., "Multiscale residual attention network for distinguishing stationary humans and common animals under through-wall condition using ultra-wideband radar," *IEEE Access*, vol. 8, pp. 121572–121583, 2020.

[69] A. Mimouna, A. Ben Khalifa, I. Alouani, A. Taleb-Ahmed, A. Rivenq, and N. Ben Amara, "LSTM-based system for multiple obstacle detection using ultra-wide band radar," in *Proc. 13th Int. Conf. Agents Artif. Intell.*, Feb. 2021, pp. 418–425. [Online]. Available: https://hal.science/hal-03195216

[70] Z. Yang, F. Shi, and H. Liang, "A portable traffic counting, speed estimation, and classification terminal using IR-UWB radar," *IEEE Sensors J.*, vol. 22, no. 13, pp. 13365–13374, Jul. 2022.

[71] W. H. Lee et al., "Non-contact sleep/wake monitoring using impulse-radio ultrawideband radar in neonates," *Front. Pediatr.*, vol. 9, Dec. 2021, Art. no. 782623. [Online]. Available: https://www.frontiersin.org/articles/10.3389/fped.2021.782623

[72] A. Sarkar and D. Ghosh, "Accurate sensing of multiple humans buried under rubble using IR-UWB SISO radar during search and rescue," *Sens. Actuators A, Phys.*, vol. 348, Dec. 2022, Art. no. 113975. [Online]. Available: https://www.sciencedirect.com/science/article/pii/S0924424722006100

[73] S. Lim, J. Jung, S.-C. Kim, and S. Lee, "Deep neural network-based in-vehicle people Localization using ultra-wideband radar," *IEEE Access*, vol. 8, pp. 96606–96612, 2020.

[74] W. H. Lee et al., "Feasibility of non-contact cardiorespiratory monitoring using impulse-radio ultra-wideband radar in the neonatal intensive care unit," *PLoS One*, vol. 15, no. 12, pp. 1–15, Dec. 2021. [Online]. Available: https://doi.org/10.1371/journal.pone.0243939

[75] G. Beltrão et al., "Contactless radar-based breathing monitoring of premature infants in the neonatal intensive care unit," *Sci. Rep.*, vol. 12, no. 1, p. 5150, Mar. 2022. [Online]. Available: https://doi.org/10.1038/s41598-022-08836-3

[76] Y. Jing et al., "Respiration detection of ground injured human target using UWB radar mounted on a hovering UAV," *Drones*, vol. 6, no. 9, p. 235, 2022. [Online]. Available: https://www.mdpi.com/2504-446X/6/9/235

[77] Z. Duan and J. Liang, "Non-contact detection of vital signs using a UWB radar sensor," *IEEE Access*, vol. 7, pp. 36888–36895, 2019.

[78] Y. Zhang, X. Li, R. Qi, Z. Qi, and H. Zhu, "Harmonic multiple loop detection (HMLD) algorithm for not-contact vital sign monitoring based on ultra-wideband (UWB) radar," *IEEE Access*, vol. 8, pp. 38786–38793, 2020.

[79] J.-Y. Park et al., "Preclinical evaluation of noncontact vital signs monitoring using real-time IR-UWB radar and factors affecting its accuracy," *Sci. Rep.*, vol. 11, no. 1, Dec. 2021, Art. no. 23602. [Online]. Available: https://doi.org/10.1038/s41598-021-03069-2

[80] X. Dang, J. Zhang, and Z. Hao, "A non-contact detection method for multi-person vital signs based on IR-UWB radar," *Sensors*, vol. 22, no. 16, p. 6116, 2022. [Online]. Available: https://www.mdpi.com/1424-8220/22/16/6116

[81] T. Zheng, Z. Chen, S. Zhang, C. Cai, and J. Luo, "MoRe-Fi: Motion-robust and fine-grained respiration monitoring via deep-learning UWB radar," in *Proc. 19th ACM Conf. Embedded Netw. Sens. Syst.*, 2021, pp. 111–124. [Online]. Available: https://doi.org/10.1145/3485730.3485932

[82] X. Jingbo, X. Xiaohong, L. Qiaowei, M. Wenbo, and Z. Fujun, "Method of extracting respiration rate and heartrate by ultra-wideband radar for human monitoring," *Sens. Mater.*, vol. 35, no. 1, pp. 103–220, 2023.

[83] C. G. Bilich, "Bio-medical sensing using ultra wideband communications and radar technology: A feasibility study," in *Proc. Pervasive Health Conf. Workshops*, 2006, pp. 1–9.

[84] S. Skaria, A. Al-Hourani, and R. J. Evans, "Deep-learning methods for hand-gesture recognition using ultra-wideband radar," *IEEE Access*, vol. 8, pp. 203580–203590, 2020.

[85] J. Maitre, K. Bouchard, C. Bertuglia, and S. Gaboury, "Recognizing activities of daily living from UWB radars and deep learning," *Expert Syst. Appl.*, vol. 164, Feb. 2021, Art. no. 113994. [Online]. Available: https://www.sciencedirect.com/science/article/pii/S0957417420307703

[86] S. Dill, E. Schreiber, M. Engel, A. Heinzel, and M. Peichl, "A drone carried multichannel synthetic aperture radar for advanced buried object detection," in *Proc. IEEE Radar Conf. (RadarConf)*, 2019, pp. 1–6.

[87] X. Liang, S. Ye, C. Song, Q. Kong, X. Liu, and G. Fang, "Enhancement of vital signals for UWB through-wall radar using low-rank and block-sparse matrix decomposition," *Remote Sens.*, vol. 16, no. 4, p. 620, 2024. [Online]. Available: https://www.mdpi.com/2072-4292/16/4/620

[88] Z. Zhang, Y. Nian, J. Chen, and M. He, "An experimental study to optimize the stepped-frequency continuous-wave radar parameters for noncontact multi-target vital sign monitoring," in *Proc. IEEE Int. Conf. Comput. Electromagnet. (ICCEM)*, 2019, pp. 1–4.

[89] W.-C. Su, M.-C. Tang, R. E. Arif, T.-S. Horng, and F.-K. Wang, "Stepped-frequency continuous-wave radar with self-injection-locking technology for monitoring multiple human vital signs," *IEEE Trans. Microw. Theory Techn.*, vol. 67, no. 12, pp. 5396–5405, Dec. 2019.

[90] J. Yang, T. Jin, C. Xiao, and X. Huang, "Compressed sensing radar imaging: Fundamentals, challenges, and advances," *Sensors*, vol. 19, no. 14, p. 3100, 2019. [Online]. Available: https://www.mdpi.com/1424-8220/19/14/3100

[91] Y. Chen, S. Wang, Y. Luo, and H. Liu, "Measurement matrix optimization based on target prior information for radar imaging," *IEEE Sensors J.*, vol. 23, no. 9, pp. 9808–9819, May 2023.

[92] H. Sadreazami, M. Bolic, and S. Rajan, "Contactless fall detection using time-frequency analysis and convolutional neural networks," *IEEE Trans. Ind. Informat.*, vol. 17, no. 10, pp. 6842–6851, Oct. 2021.

[93] S. H. Shaikh, K. Saeed, and N. Chaki, *Moving Object Detection Using Background Subtraction*. Cham, Switzerland: Springer, 2014, pp. 15–23. [Online]. Available: https://doi.org/10.1007/978-3-319-07386-6_3

[94] Y. Liu, H. An, and S. Bian, "Hilbert-Huang transform and the application," in *Proc. IEEE Int. Conf. Artif. Intell. Inf. Syst. (ICAIIS)*, 2020, pp. 534–539.

[95] L. Wang and Y. Wang, "A new signal processing algorithm for ultra-wideband radar life detection," in *Proc. Progr. Electromagn. Res. Symp. (PIERS)*, 2017, pp. 560–564.

[96] Z. Zhen and L. Fang, "Application of wavelet analysis technique in the signal denoising of life sign detection," *Phys. Procedia*, vol. 24, pp. 2124–2130, Mar. 2012.

[97] Y. E. Acar, I. Saritas, and E. Yaldiz, "An experimental study: Detecting the respiration rates of multiple stationary human targets by stepped frequency continuous wave radar," *Measurement*, vol. 167, Jan. 2021, Art. no. 108268. [Online]. Available: https://www.sciencedirect.com/science/article/pii/S0263224120308071

[98] A. Bole, A. Wall, and A. Norris, "Chapter 2—The radar system—Technical principles," in *Radar and ARPA Manual (Third Edition)*. Oxford, U.K.: Butterworth-Heinemann, 2014, pp. 29–137.

[99] M. Q. Nguyen, A. Flores-Nigaglioni, and C. Li, "Range-gating technology for millimeter-wave radar remote gesture control in IoT applications," in *Proc. IEEE MTT-S Int. Wireless Symp. (IWS)*, 2018, pp. 1–4.

[100] M. J. Oyan, S.-E. Hamran, L. Hanssen, T. Berger, and D. Plettemeier, "Ultrawideband gated step frequency ground-penetrating radar," *IEEE Trans. Geosci. Remote Sens.*, vol. 50, no. 1, pp. 212–220, Jan. 2012.

[101] B. Kim et al., "A dual-band FMCW radar for through-wall detection," in *Proc. IEEE 5th Asia-Pacific Conf. Synthetic Aperture Radar (APSAR)*, 2015, pp. 54–57.

[102] S. Indolia, A. K. Goswami, S. Mishra, and P. Asopa, "Conceptual understanding of convolutional neural network—A deep learning approach," *Procedia Comput. Sci.*, vol. 132, pp. 679–688, Jun. 2018. [Online]. Available: https://www.sciencedirect.com/science/article/pii/S1877050918308019

[103] A. Harb et al., "Diverse distant-students deep emotion recognition and visualization," *Comput. Elect. Eng.*, vol. 111, Nov. 2023, Art. no. 108963.

[104] J. Yousaf, A. M. Abed, H. Zia, E. Almajali, F. A. Tahir, and H. Rmili, "Robust deep learning-based detection and classification system for chipless arabic RFID letters," *Eng. Appl. Artif. Intell.*, vol. 122, Jun. 2023, Art. no. 106147.

[105] A. Shrestha and A. Mahmood, "Review of deep learning algorithms and architectures," *IEEE Access*, vol. 7, pp. 53040–53065, 2019.

[106] L. R. Medsker and L. Jain, "Recurrent neural networks," *Design Appl.*, vol. 5, nos. 64–67, p. 2, 2001.

[107] H. Du, T. Jin, Y. He, Y. Song, and Y. Dai, "Segmented convolutional gated recurrent neural networks for human activity recognition in ultra-wideband radar," *Neurocomputing*, vol. 396, pp. 451–464, Jul. 2020.

[108] S. Pouyanfar et al., "A survey on deep learning: Algorithms, techniques, and applications," *ACM Comput. Surveys*, vol. 51, pp. 1–36, Sep. 2018.

[109] L. Alzubaidi et al., "Review of deep learning: Concepts, CNN architectures, challenges, applications, future directions," *J. Big Data*, vol. 8, no. 1, p. 53, Mar. 2021. [Online]. Available: https://doi.org/10.1186/s40537-021-00444-8

[110] C. Zheng et al., "Deep learning-based human pose estimation: A survey," Dec. 2020, *arXiv:2012.13392*.

[111] M. Schonlau and R. Y. Zou, "The random forest algorithm for statistical learning," *Stata J.*, vol. 20, no. 1, pp. 3–29, 2020. [Online]. Available: https://doi.org/10.1177/1536867X20909688

[112] T. Sugitani et al., "Complex permittivities of breast tumor tissues obtained from cancer surgeries," *Appl. Phys. Lett.*, vol. 104, no. 25, Jun. 2014, Art. no. 253702. [Online]. Available: https://doi.org/10.1063/1.4885087

[113] M. Lazebnik, M. Okoniewski, J. H. Booske, and S. C. Hagness, "Highly accurate Debye models for normal and malignant breast tissue dielectric properties at microwave frequencies," *IEEE Microw. Wireless Compon. Lett.*, vol. 17, no. 12, pp. 822–824, Dec. 2007.

[114] T. Zheng, Z. Chen, J. Luo, L. Ke, C. Zhao, and Y. Yang, "SiWa: See into walls via deep UWB radar," in *Proc. 27th Annu. Int. Conf. Mobile Comput. Netw.*, 2021, pp. 323–336. [Online]. Available: https://doi.org/10.1145/3447993.3483258

[115] Z. Gu, X. He, G. Fang, C. Xu, F. Xia, and W. Jia, "Millimeter wave radar-based human activity recognition for healthcare monitoring robot," 2024, *arXiv:2405.01882*.

[116] A. K. Alhazmi et al., "Intelligent millimeter-wave system for human activity monitoring for telemedicine," *Sensors*, vol. 24, no. 1, p. 268, 2024. [Online]. Available: https://www.mdpi.com/1424-8220/24/1/268

[117] A. Soumya, C. K. Mohan, and L. R. Cenkeramaddi, "Recent advances in mmWave-radar-based sensing, its applications, and machine learning techniques: A review," *Sensors*, vol. 23, no. 21, p. 8901, 2023. [Online]. Available: https://www.mdpi.com/1424-8220/23/21/8901

[118] A. Haider, F. Shaukat, and J. Mir, "Human detection in aerial thermal imaging using a fully convolutional regression network," *Infrared Phys. Technol.*, vol. 116, Aug. 2021, Art. no. 103796. [Online]. Available: https://www.sciencedirect.com/science/article/pii/S1350449521001687

[119] K. R. Akshatha, A. K. Karunakar, S. B. Shenoy, A. K. Pai, N. H. Nagaraj, and S. S. Rohatgi, "Human detection in aerial thermal images using faster R-CNN and SSD algorithms," *Electronics*, vol. 11, no. 7, p. 1151, 2022. [Online]. Available: https://www.mdpi.com/2079-9292/11/7/1151

[120] T. Irshad et al., "A deep learning based human detection and tracking for security surveillance systems," *Appl. Comput. Eng.*, vol. 2, pp. 569–577, Mar. 2023.

[121] Y. Yang, P. Hu, J. Shen, H. Cheng, Z. An, and X. Liu, "Privacy-preserving human activity sensing: A survey," *High-Confidence Comput.*, vol. 4, no. 1, 2024, Art. no. 100204. [Online]. Available: https://www.sciencedirect.com/science/article/pii/S2667295224000072

[122] A. A. Aguileta, R. F. Brena, O. Mayora, E. Molino-Minero-Re, and L. A. Trejo, "Multi-sensor fusion for activity recognition—A survey," *Sensors*, vol. 19, no. 17, p. 3808, 2019. [Online]. Available: https://www.mdpi.com/1424-8220/19/17/3808

[123] D. Koutrintzes, E. Spyrou, E. Mathe, and P. Mylonas, "A multimodal fusion approach for human activity recognition," *Int. J. Neural Syst.*, vol. 33, no. 1, 2023, Art. no. 2350002. [Online]. Available: https://pubmed.ncbi.nlm.nih.gov/36573880/